Magnetic resonance imaging techniques for the assessment of the control mechanisms underlying gastric motor function

A dissertation submitted to the

SWISS FEDERAL INSTITUTE OF TECHNOLOGY ZURICH

for the degree of

Doctor of Natural Science

presented by

Henryk Michael Faas

Dipl. Phys. ETH

born January 25, 1970

citizen of Karlsruhe (Germany)

accepted on the recommendation of

Prof. Dr. P. Boesiger, examiner

Prof. Dr. M. Fried, co-examiner

PD Dr. P. Enck, co-examiner

Zürich, 1999

Zusammenfassung

Das vegetative Nervensystem kontrolliert lebenswichtige Funktionen wie die Regulation der Nährstoffaufnahme, des Stoffwechsels oder des kardiovaskulären Systems. Vegetative Prozesse unterliegen nicht der willkürlichen Kontrolle und werden im Regelfall auch nicht bewusst wahrgenommen. Wie diese Regulation und Kontrolle beim Menschen erreicht wird, ist noch unzureichend verstanden. Ein Grund liegt sicher in der Schwierigkeit, geeignete physiologische Parameter zu identifizieren, und in methodischen Beschränkungen, die komplexe Interaktion verschiedener physiologischer Systeme zu untersuchen. Die vorliegende Arbeit stellt einen Versuch in diese Richtung dar. Ziel war die Untersuchung grundlegender Regelmechanismen am Beispiel der glatten Magenmuskulatur. Dabei folgten die Experimente einem gemeinsamen Aufbau: Die antrale kontraktile Aktivität wurde als Antwortfunktion auf einen definierten peripheren oder zentralen Reiz betrachtet. Zur Beobachtung dieser Reaktion wurden Magnetresonanzbildgebungsverfahren (MRI) entwickelt. Zunächst wurde durch die Kombination von MRI und hochauflösender Druckmessung die Änderung der antroduodenalen Motorfunktion bei Stimulation duodenaler Nährstoffrezeptoren untersucht. Es konnte gezeigt werden, dass dabei die zeitliche Koordination der Kontraktionsaktivität und der antroduodenale Druckgradient eine zentrale Rolle einnehmen. Durch Einsatz des Motilinagonisten Erythromycin wurde diese normale physiologische Funktion verändert, wobei Episoden starker Kontraktionsaktivität auftraten. Dass sich MRI verglichen mit Manometrie als wesentlich zuverlässiger zur Detektion antraler Kontraktionen erwies, muss bei der Interpretation von Druckdaten berücksichtigt werden. Gegenstand eines weiteren Teils der Arbeit war die Frage, wie die Aktivität der glatten Muskulatur durch das Zentralnervensystem moduliert wird. Als externer Reiz wurde ein Gefühl der Eigenrotation durch Bewegung des Sichtfeldes erzeugt. Es konnte gezeigt werden, dass unter diesen Bedingungen eine deutliche Hemmung der antralen Kontraktionsaktivität auftritt, die jedoch unabhängig von der Intensität der subjektiven Wahrnehmung der Versuchspersonen aufzutreten scheint. Gegenwärtig wird untersucht, welche zentralen Mechanismen für diese Auswirkungen auf das vegetative System verantwortlich sind. Ein weiterer Aspekt der Arbeit war die Identifizierung der Mechanismen, die für die Ausbreitung von oral verabreichten Medikamenten vor Absorption im

Gastrointestinaltrakt verantwortlich sind. Dazu wurde ein kolloidales Medikamentenmodell entwickelt, dessen Ausbreitungsdynamik durch den Einschluss eines MR-Kontrastmittels in eine Liposomhülle verfolgt werden konnte. Dies könnte wertvolle Hinweise für die Optimierung galenischer Formulierungen liefern.

Summary

The autonomic nervous system performs crucial tasks such as the control of the respiratory and cardiovascular system or the regulation of gastrointestinal function. Visceral functions are not subject to voluntary control and are usually not consciously perceived. Despite intensive research on how this regulation is achieved, a great amount of uncertainty prevails. Partly responsible for this are the difficulty in identifying suitable physiological parameters and methodological limitations when trying to assess the complex interaction between different physiological systems. This work aimed to address these shortcomings. The experiments followed a common basic structure: a stimulus was applied either peripherally or centrally and, disregarding the cascade of events in between, the final response was assessed by imaging antral contractile activity by dynamic MRI. For this purpose, magnetic resonance imaging techniques were developed. In the first part, the response of antral activity to caloric stimulation of duodenal nutrient receptors was studied by a combination of MR imaging and high-resolution manometry to obtain complementary information on pressure and wall motion. We found that temporal and spatial coordination of contractile activity and the antroduodenal pressure gradient play a crucial role for normal gastric function. This normal function was altered by the motilin agonist erythromycin that induced episodes of strong contractile activity. In the second part of the work, we investigated the role of the brain in the modulation of gastric motor activity. The external stimulus was illusory self-motion elicited by circular vection. We observed a characteristic inhibition of antral contractile activity, largely independent of the centrally generated symptoms of motion sickness. Currently it is investigated, which central mechanisms are responsible for this effect on the vegetative system. An additional aspect of this work was the identification of the mechanisms underlying the distribution of orally administered drugs in the gastrointestinal tract. For this purpose, we developed a colloidal drug model, whose distribution dynamics could be followed by enclosing an MR contrast agent in a phospholipid vesicle. This provides valuable information for the optimisation of galenic preparations. In summary, MRI offers unique possibilities to study visceral regulatory systems, as demonstrated on the example of gastric function, thus allowing new insights into the underlying

mechanisms. In addition, MRI can be expected to make important contributions to the design of orally administered drugs.

Contents

Chapter 1

Introduction

Like most visceral processes, gastric function is closely regulated, but rarely gets to our immediate attention. This regulation is accomplished by a hierarchical organization of the different control mechanisms involved. The most basic functions and reflexes, e.g. peristaltic contractions, are embedded in the enteric nervous system, an extensive neural network situated in the gut wall. These basic activities are modulated from various sources by humoral mechanisms and through the autonomic nervous system. The regulatory mechanisms underlying gastric function are far from being resolved, particularly in humans, partly because of a lack of suitable techniques for its assessment. One aim of this work was therefore to develop magnetic resonance imaging (MRI) methods to assess regulatory control mechanisms underlying gastric motor function. Improved knowledge of these mechanisms is also important for the design of orally administered drugs, whose bioavailability is strongly affected by the behavior of the formulation in the gastrointestinal tract. Since current understanding of the release and distribution of drugs in the gastrointestinal tract is scanty, we aimed further to develop a method to monitor the intragastric distribution of a drug model by MRI.

Antroduodenal contractile activity

In the postprandial state, the contractile motor activity in the gastroduodenal region is largely determined by feedback from small intestinal chemo- and mechanoreceptors. Infusion of nutrients into the duodenum during emptying of liquid leads to a drastic change in gastroduodenal motor activity by suppression of antral pressure waves, stimulation of phasic pyloric pressure events and an increase in basal pyloric tone [1, 2]. However, the role of the different mechanisms responsible for the delivery of nutrients to the small intestine (proximal and distal gastric contractile activity, pyloric resistance

1

and duodenal motor activity) is unclear. While no single factor could be identified to exert a dominant control [3, 4], the concerted action of the different motor mechanisms appears to be required for the control of gastric emptying. This hypothesis is further supported by the observation that the stomach is capable of reorganizing its motor activity when individual motor components fail, before compromising the nutrient load delivered to the small intestine [5]. It has been shown that the timing of antral, pyloric and duodenal contractile events strongly influences transpyloric flow [4]. Transpyloric flow is pulsatile [6, 7], and depends on the spatial and temporal organization of the motor events in the proximal and distal stomach, the duodenum and the resistive force of the pyloric sphincter [5, 8].

Studies on the mechanisms underlying the regulation of gastric emptying ideally should include a simultaneous assessment of all motor components correlated with transpyloric flow on a second-to-second basis and should take into account the temporal and spatial relationship of these mechanisms [8]. Since conclusions drawn from animal studies can hardly be extrapolated, there is a need for combined techniques to assess the individual motor components - wall motion and intraluminal pressure - and, as the outcome variable, transpyloric flow in humans. Such studies have not been performed due to methodological limitations. So far, only two studies combined an imaging modality, videofluoroscopy and scintigraphy respectively, with intraluminal manometry in humans [9, 10]. Much of the current knowledge about the relationships between individual motor components arises from the assessment of intraluminal pressures. Perfusion manometry allows to study antral, pyloric and duodenal pressures simultaneously [1, 8], but does not directly reflect wall motion. The motion of the luminal wall can be assessed by videofluoroscopy with good spatial and temporal resolution [11]. However, the technique only yields 2D projections so that gastric emptying cannot be quantified, and its application is severely limited by the radiation burden involved. Ultrasonography has been developed to assess wall motion and gastric emptying [12, 13, 14]. The drawbacks are that, for functional studies, ultrasonography is restricted to liquid meals, can only partly image the gastric lumen and is subject to artifacts from air. It is the only method so far to quantify transpyloric flow in humans, even though with limited precision [13]. Magnetic resonance imaging methods have been used to quantify gastric emptying [15, 16] and wall motion [17, 18]. MRI studies so far have focused on antral

motility, while the gastroduodenal region has not been assessed. The reason is that navigation to the area of interest is still difficult compared to ultrasonography and that temporal resolution is low. Imaging of the abdomen, where respiratory and peristaltic motion limits acquisition times, poses particular demands on MR imaging techniques. Having no trigger available as in cardiac MRI, imaging of gastric motor activity requires rapid data acquisition balanced against sufficient signal to noise intensity in order to visualize complex mechanical processes.

The aim of the first part of this work was therefore to develop an MRI method to assess intraluminal pressures concurrently with gastric wall motion and the rate of gastric emptying. This technique has then been applied to study the motor mechanisms during intraduodenal lipid infusion before and after administration of the motilin agonist erythromycin. In addition, we aimed to develop new imaging strategies for the assessment of gastroduodenal function.

Sensory conflicts and the central modulation of gastric motility

The role that the brain exerts in the control of gastric function has been appreciated since the beginning of the century, when it was shown that emotional states evoked by external stimuli can have a profound impact on motor patterns in the GI tract [19, 20]. Since then, a variety of environmental stimuli have been demonstrated to affect gastric motility. Cold pressor stress, where subject's hand is repeatedly exposed the to 4 °C cold water, is associated with antral inhibition and changes in pyloric and duodenal motility [21] and labyrinthine stimulation delays gastric emptying [22]. Motion stimuli also have an effect on gastric function [23, 24]. Vection has been used to investigate the effect of illusory self-motion on gastric function and to understand the nature of the accompanying physiological symptoms of motion sickness [25, 26].

Illusory self-motion can be experienced by gazing from a bridge onto a river or looking at a train take off from an adjacent track. Since the vestibular system can only detect acceleration and deceleration, information on constant motion has to rely completely on the visual system. Therefore, self-motion can be induced by moving the surround of a stationary subject e.g. by a rotating optokinetik drum (circular vection). A recent study using PET investigated the cortical areas involved in the visual perception of self-

motion [27]. It was shown that visual motion stimulation not only activates bilaterally a parieto-occipital visual area but also deactivates the parieto-insular vestibular cortex. The authors found a positive correlation between the perceived intensity of circular vection and the relative changes in cerebral blood flow in parietal and occipital areas. They concluded that reciprocal visual-vestibular interaction acts as a multisensory mechanism for self-motion perception, shifting the dominant sensorial weight from one sensory modality to the other.

The mechanisms underlying the physiological symptoms of motion sickness are not understood, even though there has been intensive research motivated by the fact that motion sickness represents the most critical health problem during the first days of space flight. A general concept for the explanation of motion sickness has been proposed by Reason [28]. Motion sickness results when there is a mismatch between predicted and actual sensory inputs. In case of circular vection, the incoming somatosensory information from the visual, vestibular and proprioceptive system is inconsistent with previous sensory-motor experiences. This visual-vestibular conflict signal triggers the different mechanisms mediating the symptoms of motion sickness. Adaptation or habituation to the stimulus will decrease the symptoms over long-term or repeated exposure to the stimulus. The physiological correlates of motion sickness include various effects on cardiovascular and respiratory system as well as the gastrointestinal and neuroendocrine system [29].

Changes in gastric function have been shown to occur under circular vection. A close relationship was found between the incidence of motion sickness symptoms and gastric rhythm disturbances determined by electrogastrography (EGG) [25]. However, intensity of the EGG is not directly correlated with the contractile activity of the stomach wall [25]. Vection slows gastric emptying in susceptible subjects [30], an effect, which was not closely related to the observed intensity of symptoms. Since, as described above, gastric emptying is the result of a variety of motor components, its assessment alone does not allow to derive information on the effects of vection on gastric motility. So far, no direct observation of gastric contractile activity during experience of vection has been reported. Thus, it remains subject of debate whether changes in gastric activity are the cause of the motion sickness symptoms or just occur coincidentally.

The aim of the second part of the work was therefore to investigate by MRI the response of gastric motility and gastric emptying to an external vection stimulus.

Monitoring intragastric drug distribution

The behaviour of orally administered drugs in the gastrointestinal tract strongly influence their bioavailability. This is particularly true for enzymes that rely on substrates in the GI tract or if timing and location of drug absorption is important. Only little is known about the mechanisms governing the distribution of a given galenic form in the gastrointestinal tract. As a consequence of the growing complexity of drugs, suitable methods are needed to monitor the release of drugs from specific galenic preparations within the gastrointestinal tract in order to understand the relevant factors influencing their distribution. Drug formulations can then be optimized with respect to their behaviour in the gastrointestinal tract.

Gamma scintigraphy, where the drug is labeled with radioisotopes, has been used for this purpose [31]. Drawbacks of this technique are the radiation burden involved and the lack of three-dimensional information on drug distribution and the anatomical environment. Magnetic resonance imaging (MRI) would be an attractive alternative or supplementary tool to gamma scintigraphy, since the technique provides 3D information, is free of ionizing radiation and allows the assessment of gastric motor function. In the rat stomach, the fate of a solid dosage form has recently been visualized by MRI [32]. No studies have yet been performed using MRI to follow the intragastric distribution of a realistic drug model that resembles galenic formulations in humans.

The aim of the third part of the work was to develop a method to visualize the distribution of Gd-DOTA-labelled liposomes as a drug model in the human stomach after ingestion of a liquid or a solid meal.

References

1. Heddle R, Dent J, Toouli J, Read NW. Topography and measurement of pyloric pressure waves and tone in humans. Am J Physiol 1988;255:G490-7.

2. Heddle R, Fone D, Dent J, Horowitz M. Stimulation of pyloric motility by intraduodenal dextrose in normal subjects. Gut 1988;29(10):1349-57.

3. Heddle R, Miedema BW, Kelly KA. Integration of canine proximal gastric, antral, pyloric, and proximal duodenal motility during fasting and after a liquid meal. Dig Dis Sci 1993;38(5):856-69.

4. Malbert CH, Serthelon JP, Dent J. Changes in antroduodenal resistance induced by Cisapride in conscious dogs. Am J Physiol 1992;263:G202-8.

5. Malbert CH, Mathis C, Laplace JP. Vagal control of pyloric resistance. Am J Physiol 1995;269:G558-69.

6. Malbert CH, Ruckebusch Y. Relationships between pressure and flow across the gastroduodenal junction in dogs. Am J Physiol 1991; 260:G653-7.

7. Houghton LA, Read NW, Heddle R, Maddern GJ, Downton J, Toouli J, Dent J. Motor activity of the gastric antrum, pylorus, and duodenum under fasted conditions and after a liquid meal. Gastroenterology 1988;94(6):1276-84.

8. Horowitz M, Dent J, Fraser R, Sun W, Hebbard G. Role and integration of mechanisms controlling gastric emptying. Dig Dis Sci 1994;39(12 Suppl):7S-13S.

9. Tougas G, Anvari M, Dent J, Somers S, Richards D, Stevenson GW. Relation of pyloric motility to pyloric opening and closure in healthy subjects. Gut 1992;33(4):466-71.

10. Jones K, Edelbroek M, Horowitz M, Sun WM, Dent J, Roelofs J, Muecke T, Akkermans L. Evaluation of antral motility in humans using manometry and scintigraphy. Gut 1995;37(5):643-8.

11. Anvari M, Dent J, Malbert C, Jamieson GG. Mechanics of pulsatile transpyloric flow in the pig. J Physiol Lond 1995;488:193-202.

12. King PM, Adam RD, Pryde A, McDicken WN, Heading RC. Relationships of human antroduodenal motility and transpyloric fluid movement: non-invasive observations with real-time ultrasound. Gut 1984;25(12):1384-91.

13. Hausken T, Odegaard S, Matre K, Berstad A. Antroduodenal motility and movements of luminal contents studied by duplex sonography. Gastroenterology 1992;102(5):1583-90.

14. Gilja OH, Detmer PR, Jong JM, Leotta DF, Li XN, Beach KW, Martin R, Strandness DE. Intragastric distribution and gastric emptying assessed by three-dimensional ultrasonography. Gastroenterology 1997;113(1):38-49.

15. Schwizer W, Maecke H, Fried M. Measurement of gastric emptying by magnetic resonance imaging in humans. Gastroenterology 1992;103(2):369-76.

16. Feinle C, Kunz, P, Boesiger, P, Fried, M, Schwizer, W. Scintigraphic validation of a magnetic resonance imaging to study gastric emptying in humans. Gut 1999;44:106-111.

17. Schwizer W, Fraser R, Borovicka J, Asal K, Crelier G, Kunz P, Boesiger P, Fried M. Measurement of proximal and distal gastric motility with magnetic resonance imaging. Am J Physiol 1996;271:G217-22.

18. Kunz P, Crelier GR, Schwizer W, Borovicka J, Kreiss C, Fried M, Boesiger-P. Gastric emptying and motility: assessment with MR imaging--preliminary observations. Radiology 1998;207(1):33-40.

19. Pavlov I. The work of digestive glands. London: Griffin, 1910.

20. Cannon WB. The influence of emotional states on the functions of the alimentary canal. Am J Med Sci 1909;137:480-487.

21. Fone DR, Horowitz M, Maddox A, Akkermans LM, Read NW, Dent J. Gastroduodenal motility during the delayed gastric emptying induced by cold stress. Gastroenterology 1990;98:1155-61.

22. Thompson DG, Richelson E, Malagelada JR. Perturbation of gastric emptying and duodenal motility through the central nervous system. Gastroenterology 1982; 83(6):1200-1206.

23. McDonough MC, Schneider M. The effect of motion on the roentgenographic appearance of the stomach and small bowel. Gastroenterology 1944;2:32-45.

24. Wood MJ, Wood CD, Manno JE, Manno BR, Redetzki HM. Nuclear medicine evaluation of motion sickness and medications on gastric emptying time. J Clin Invest 1987:22:877-882.

25. Stern RM, Koch KL, Leibowitz HW, Lindblad IM, Shupert CL, Stewart WR. Tachygastria and motion sickness. Aviat Space Environ Med 1985;56(11):1074-7.

25. Stern RM, Koch KL, Stewart WR, Lindblad IM. Spectral analysis of tachygastria recorded during motion sickness. Gastroenterology 1987; 92(1):92-7.

26. Koch KL, Stern RM, Vasey MW, Seaton JF, Demers LM, Harrison TS. Neuroendocrine and gastric myoelectrical responses to illusory self-motion in humans. Am J Physiol 1990;258:E304-10.

27. Brandt T, Bartenstein P, Janek A, Dieterich M. Reciprocal inhibitory visual-vestibular interaction. Visual motion stimulation deactivates the parieto-insular vestibular cortex. Brain 1998;121:1749-58.

28. Reason JT. Motion sickness adaptation: a neural mismatch model. J Royal Soc Med 1974;71:819-829.

29. Harm D. Physiology of motion sickness symptoms. In Crampton G (Ed.). Motion and space sickness. Boca Raton: CRC Press, 1990:153-177.

30. Reid K, Grundy D, Khan MI, Read NW. Gastric emptying and the symptoms of vection-induced nausea. Eur J Gastroenterol Hepatol 1995;7:103-8.

31. Wilson CG, McJury M, O'Mahony B, Frier M., Perkins A.C. Imaging oily formulations in the gastrointestinal tract. Advanced Drug Delivery Reviews 1997;25:91-101.

32. Christmann V, Rosenberg J, Seega J, Lehr C.M. Simultaneous in vivo visualisation and localisation of solid oral dosage forms in the rat gastrointestinal tract by magnetic resonance imaging (MRI). Pharm Res 1998; 14: 1066-1072.

Chapter 2

Combining MRI and manometry to assess antroduodenal motor activity

H. Faas [1], G. Hebbard [2], JG Brasseur [3], C. Feinle [4], P. Kunz [1], K. Indireshkumar [3], J. Dent [2], P. Boesiger [1], M. Fried [4], W. Schwizer [4]

[1] Biophysics Division, Institute of Biomedical Engineering and Medical Informatics, University and ETH Zurich, [2] Royal Adelaide University Hospital, Adelaide, Australia, [3] Department of Mechanical Engineering, Pennsylvania State University, Pennsylvania, USA, [4] Department of Gastroenterology, University Hospital Zurich, Switzerland

Abstract

Background/Aims: Understanding of the control mechanisms underlying gastric motor function is limited, in part due to methodological shortcomings in its assessment. The aim of this study was to develop a combined magnetic resonance imaging and manometry technique to obtain detailed information on pressure geometry relations and apply this to study the effect of duodenal nutrient stimulation and intravenously administered erythromycin.

Methods: Antral contractile activity was followed by combined dynamic magnetic resonance imaging (MRI) and antroduodenal high-resolution manometry (20 pressure ports) in 7 healthy subjects. Gastric volume was determined by MRI at fixed intervals. Stainless steel markers on the catheter allowed tracking of the assembly. After intragastric administration of 600 ml 20 % glucose solution, motility was assessed for 30 min under intraduodenal nutrient infusion, before the stomach was filled again. Thereafter, erythromycin was infused intravenously and the protocol continued for a further 15 min.

Results: All contraction waves were antegrade and no lumen occlusive contractions were observed in the antrum (lumen occlusion: 47 ± 14 %). The propagation speed of these peristaltic contraction waves was 2.5 ± 1.3 mm/s. 82 % (51/62) of all observed contraction waves were detected manometrically. 49 % of all contractile events (241/496) were associated with a detectable pressure event. The degree of lumen occlusion of the contractile events that had no observed pressure change was $47 \pm 15\%$. After erythromycin, episodes of strong antroduodenal contractions were observed, but antral activity was highly variable between subjects.

Conclusions: The combined MRI and manometry technique introduced in this study allows correlation of antroduodenal wall motion and pressure. A detailed knowledge of antroduodenal mechanics is fundamental to an understanding of the underlying control mechanisms.

Introduction

The control of nutrient liquid emptying is strongly influenced by feedback signals from small intestinal receptors. Intraduodenal lipid infusion slows gastric emptying, stimulates tonic and phasic pyloric motor activity and suppresses antral pressure waves[1]. Erythromycin, a motilin agonist, has been shown to accelerate pathologically delayed gastric emptying [2]. These effects are attributed primarily to increased antral activity with stimulation of distinctive high pressure waves, which sweep aborad along the distal stomach, and to suppression of localized pyloric motor activity [3]. The contribution of each of these mechanisms to the acceleration of gastric emptying have, however, not been identified.

The deficiencies in our current understanding of the mechanics of antropyloroduodenal motor function contributing to gastric emptying in humans can be attributed largely to technical difficulties in the simultaneous assessment of gastric emptying, gastric wall motion and intraluminal pressures. The majority of studies so far has relied exclusively on the measurement of one of these variables. Gastric scintigraphy has been used most extensively [4], but has poor temporal resolution. Luminal manometry has good temporal resolution, but the relationship between pressure patterns and transpyloric flow has not yet been established. As the relationships between the mechanical factors that determine gastric emptying are complicated, the ability to simultaneously record gastric wall motion and intraluminal pressures on a second to second basis would be expected to add important information to that gained from measurement of pressure alone. With magnetic resonance imaging, it is now feasible to combine real-time gastric imaging and intraluminal pressure measurement to overcome the shortcomings of current techniques [5,6]. The imaging technique should provide three dimensional information since the anatomy of the distal stomach and duodenum cannot be displayed completely by techniques relying on imaging in a single plane (e.g. fluoroscopy, ultrasound). Previous applications of magnetic resonance imaging techniques assessed gastric motor function in single planes [7]. The recent development of high speed MR imaging techniques with image acquisition in multiple planes now enables real-time three-dimensional data acquisition. Furthermore, advances in water-perfused high-resolution

manometry capable of measuring small pressure gradients have made this technique especially well suited for the analysis of antropyloric mechanics.

In this chapter we report the development of a technique combining manometry and MRI to evaluate the pressure-geometry relationships of the antropyloroduodenal region. A quantitative analysis of the pressure data is presented in chapter 3.

Methods

Subjects

Seven healthy subjects (5 m, 2 f; 23 to 45 years) with no prior history of gastrointestinal disease participated in the study. All subjects gave written informed consent, and the study protocol was approved by the Ethics Committee of the Department of Internal Medicine at the University Hospital Zurich.

Experimental protocol

The experimental protocol is shown in Figure 1a. Subjects attended the laboratory after an overnight fast. The manometric assembly, which had a chain of 19 recording sideholes spaced at 3 mm intervals (Figure 1b) was inserted through an anaesthetised nostril and positioned across the pylorus using previously validated transmucosal potential difference criteria [8]. The position of the catheter was controlled visually by two MR markers on both sides of the pressure-sensitive zone. A second tube (inner diameter 1.5 mm, outer diameter 2.5 mm), which ran alongside the manometric assembly ended in the stomach and was used for intragastric infusions. An intravenous catheter for the infusion of placebo (saline solution) or erythromycin (Erythrocine®, Abbot, Switzerland) was inserted into the antecubital fossa. After phase III of the interdigestive migrating motor complex (MMC), an intraduodenal nutrient liquid infusion (equal volumes of 25 % dextrose and a 10 % lipid emulsion (1.1 kcal/ml, Intralipid®, Kabi-Vitrum, Stockholm, Sweden)) was started at a rate of 2 ml/min (2.1 kcal/min). This rate was maintained throughout the study. The subject was placed in the MR scanner supine at 30° towards the left lateral position to ensure filling of the antrum. Isotonic saline solution (750 ml, marked with Gd-DOTA 600 μM Dotarem®, Laboratoire Guerbet, Aulnay-sous-Bois, France) as a paramagnetic MRI contrast agent

was infused over 4 min through the gastric tube. Antropyloroduodenal pressures were recorded throughout the study.
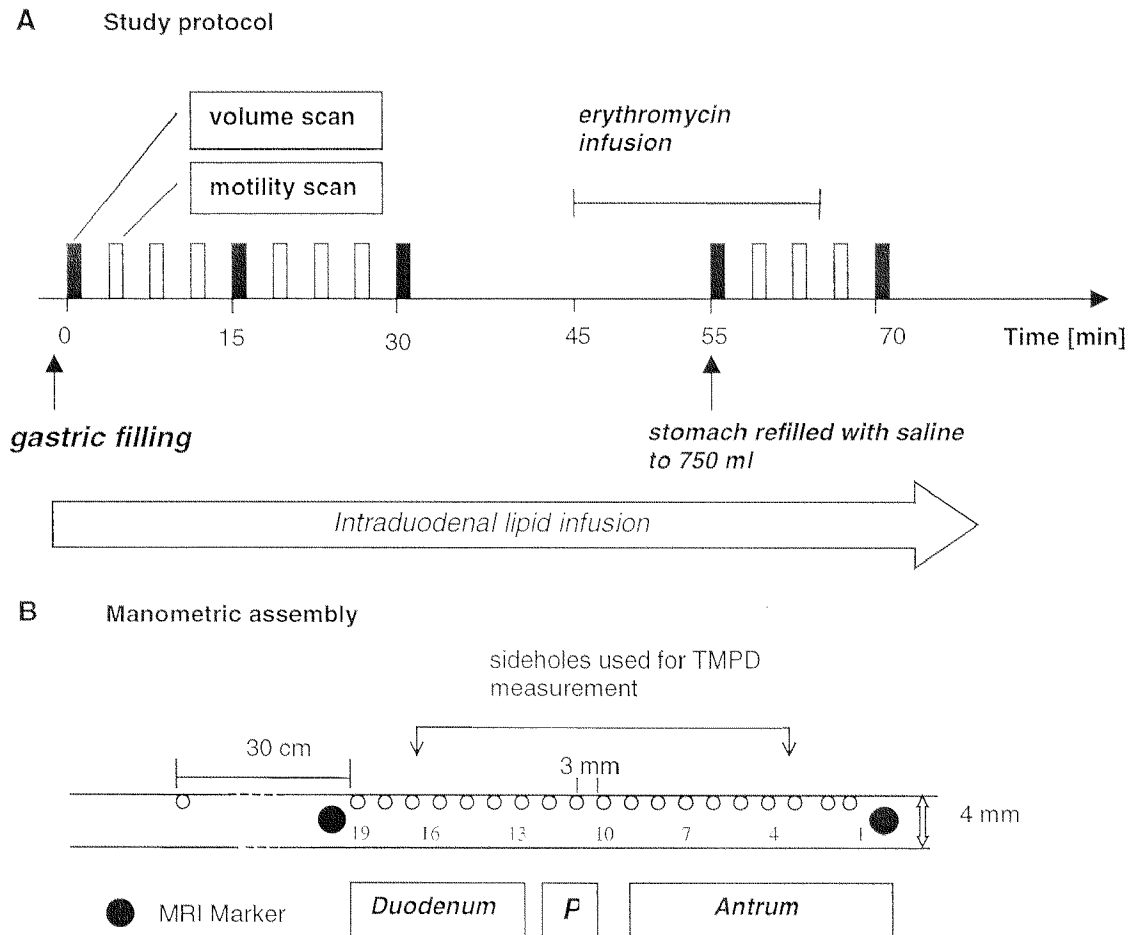
A   Study protocol

B   Manometric assembly

Figure 1: a) Study protocol: a series of four MRI scans, a 'volume scan' to measure intragastric liquid volume and three 'motility scans' to assess antroduodenal wall motion, was performed three times. Prior to the third series, erythromycin was administered intravenously. Pressures were recorded continuously throughout the study and an intraduodenal infusion was maintained at 2.1 kcal/min. **b) Manometric assembly:** The arrangement of the perfused sideholes and the markers, which indicated the zone of pressure recording sideholes of the assembly in the MR images. TMPD recording was used to aid correct positioning of the catheter across the gastroduodenal junction.

Part 1: Immediately following the intragastric saline infusion, an MR scan was performed to measure the intragastric liquid volume ('volume scan'). This was followed by three dynamic MR scans of 90 s duration each, to assess gastric motility ('motility scan'). This basic sequence was repeated twice at 15 min intervals (total 30 min).

Part 2: At 40 min, erythromycin (200 mg) was given as i.v. infusion over 20 min. At 45 min, another 500 – 750 ml isotonic saline solution was infused and two more sequences of volume and motility scans were performed for a further 30 min. Since after i.v. infusion of erythromycin the gastric lumen was almost empty within 15 min, only the first 15 min of data were analysed. The timings and other details of the experimental setup are given in Figure 1.

Magnetic resonance imaging

All studies were performed in a 1.5 Tesla whole body imager (Philips Gyroscan ACS-NT, Best, The Netherlands). Two different types of scans were used: (1) a scan to determine the amount of liquid in the gastric lumen ('volume scan') and (2) a scan to assess gastric wall motion in three dimensions ('motility scan').

Volume scan: Intragastric liquid volume was measured with a previously described method [9]. Briefly, a Turbo Spinecho scan (transverse slice orientation, echo time TE = 12 ms, repetition time TR = 576 ms, flip angle 90°) with 24 contiguous slices (7.5 mm slice thickness) was performed over 60 s. The in-plane resolution was 1.5 mm (matrix size: 256 x 256 pixels, field of view: 380 mm). To avoid motion artifacts, the scan was divided into four measurement periods of 15 s each,and the subjects were asked to hold their breath in expiration during the length of these measurements.

Motility scan: A dynamic scan was designed to assess 3D wall motion in the antropyloroduodenal area and to track the position of the manometric assembly markers (see below), in order to determine the exact position relative to the pylorus and antrum. Over 90 s, seven slices were acquired each second using a multislice gradient echo echo planar (EPI) sequence (coronal slice orientation, EPI factor 5, TE = 5 ms, TR = 81 ms, flip angle: 20°, matrix size: 128 ·128 pixels, Field of view: 400 mm, resolution: 3

mm, slice thickness: 7 mm). The scan was triggered by a signal from the computer, which acquired the manometric data, so MRI and manometry data were synchronised precisely.

Manometric technique

Pressures were recorded with a perfusion manometry system along a 20 channel, silicone rubber manometric assembly (Figure 1b; 0.4 mm inner diameter for the reording channnnels, sidehole spacing: 3 mm, perfusion rate 0.08 ml/min, perfusion pump driving pressure: 1 atm, preflushed with CO_2; Dentsleeve, Parkside, Australia). The system had a pressure response rate of 150 mmHg/s or greater on sidehole occlusion. 19 channels were used for pressure recordings with ports spaced 3.3 mm apart along a 6 cm segment of the assembly to monitor pressures in the antropyloroduodenal region. Sideholes 3 and 17 were perfused with normal saline from separate reservoirs and transmucosal potential difference (TMPD) was measured concurrently with manometry to aid the positioning of the catheter across the pylorus. Manometric data were recorded at 8 samples/min. Transducer drift was corrected every 15 min using an underwater reference, and measurement uncertainty was minimized to within 0.5 mmHg. A larger (0.9 mm diameter) channel in the assembly, which opened into the duodenum 14 cm from the pylorus, was used to deliver the intraduodenal nutrient infusion.

Data Analysis

Terminology: The term 'wave' is used to imply propagation between at least two points of observation. 'Motility' is used as a general term and refers to motor function as measured by either method, manometry or MRI. Individual wall indentations are called *contractile events* (contractions). A spatial progression of contractile events in time is defined as a *contraction wave*. Pressure increases at least 5 mmHg above baseline (see below) in a single manometric channel were defined as *pressure events*. Pressure events showing a progression in time over at least two manometric channels are called *pressure waves*.

MRI: Gastric emptying was assessed by measuring gastric volume every 15 minutes. In all 24 slices of a volume scan, the contour of the stomach content was outlined semi-

automatically. These areas were multiplied by the slice thickness and added to obtain the intragastric volume.

To analyse antral contractions, MR motility scans at each time point were evaluated for average speed of progression of the contraction, average degree of lumen occlusion and average distance from the pylorus. The degree of occlusion of the gastric lumen by a contraction at any time point was measured manually and defined as the smallest distance between opposite sides of the gastric wall in the contracted state in relation to the uncontracted state, expressed as a percentage.

To relate these geometrical variables to changes of pressure, proximal and distal markers as well as the course of the assembly in the antropyloric region were identified manually in each image of a series of dynamic scans relative to the location of the pylorus. This was carried out without reference to the pressure data. The spatial location of pressure events and wall motion were defined as the points where the assembly and a virtual line connecting the opposing antral wall indentations intersected. Contractions were therefore characterised by their position relative to the assembly, their speed, propagation and their degree of lumen occlusion. A contraction wave was defined antegrade if its propagation speed (determined by a linear fit of the displacement over time curve) exceeded 0.5 mm/s.

Manometric data: The pressures recorded included a hydrostatic pressure component due to the differences in height between the subject and the manometric transducers as well as a component corresponding to intraabdominal pressure. All pressures were expressed relative to a baseline pressure defined as the 5th centile of the pressure values in channel 19 of the manometric assembly during the pre-erythromycin period. This channel was always in the duodenum. Recordings were only analysed when the TMPD readings indicated that the assembly was correctly positioned across the pylorus.

Pressure events: During dynamic scan periods, the manometric data were subdivided in time into blocks of eight digitised values corresponding to the acquisition time of a single MR image (1 s). Since the resolution of the MRI was on the order of the manometric sidehole spacing (3 mm), the highest pressure value within the 1 s time

frame over the tracked MR image and the two adjacent pressure channels was chosen as the pressure event corresponding to the wall indentation.

Continuous pressure activity: When the image analysis and the tracking of the manometric assembly allowed assignment of specific manometric channels to the pylorus, pressures recorded from all channels proximal to the pyloric channels were used to calculate mean antral pressure, all channels distal to the pylorus yielded the mean duodenal pressure, and the three pyloric channels itself the mean pyloric pressure.

Pressure events and waves: A software program was developed to automatically detect antral pressure events and waves under visual control (manometric data displayed as contourplots). The area under the curve was defined in each antral channel as the area under the pressure vs. time curve during pressure events. The area under the curve was calculated relative to antral baseline, and the result was scaled to a total time period of 15 min for each study period. The channel with maximum area under the curve (AUC) was used to distinguish levels of antral pressure activity between subjects. Furthermore, the frequency of pressure waves was calculated.

Statistics

Data were analysed by t-test (significance level $p < 0.05$, tendency defined as $0.05 < p < 0.1$) and are presented as means $\pm$ SD, unless stated otherwise.

Results

Magnetic resonance imaging: The number of contraction waves observed was 62, the total number of contractile events 635. All contraction waves (Figure 2a) were antegrade and no lumen-occlusive contractions were observed in the antrum (lumen occlusion: 47 ± 14 %). The propagation speed of these peristaltic contraction waves was 2.5 ± 1.3 mm/s. The median gastric emptying rate was 12.0 ml/min for the first 15 min (4.2 – 17.8 ml/min) and 9.3 ml/min for the second 15 min (4.5 – 10.6 ml/min). After erythromycin, strong contractions (Figure 2 b) occurred in all subjects, so that the

position of the manometric assembly and individual contractions could not be tracked. Gastric emptying after erythromycin occurred at 20.3 ml/min (11.0 – 39.1 ml/min).
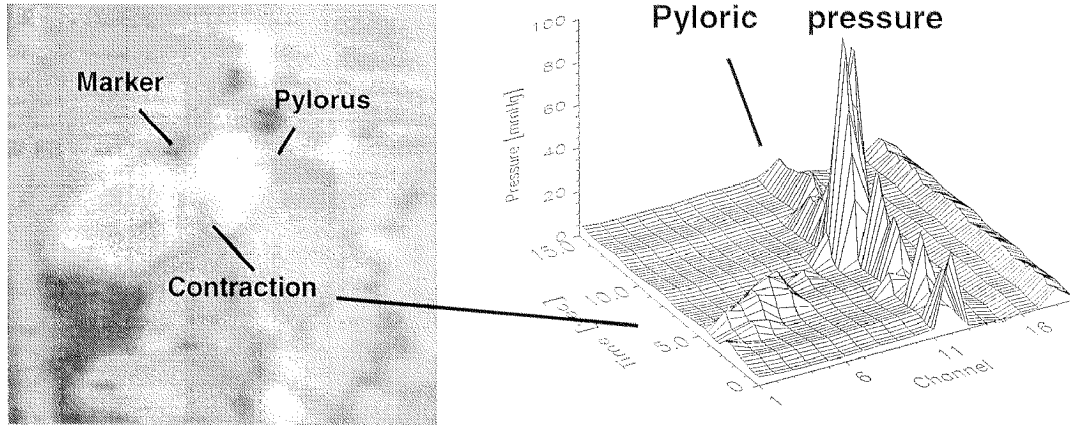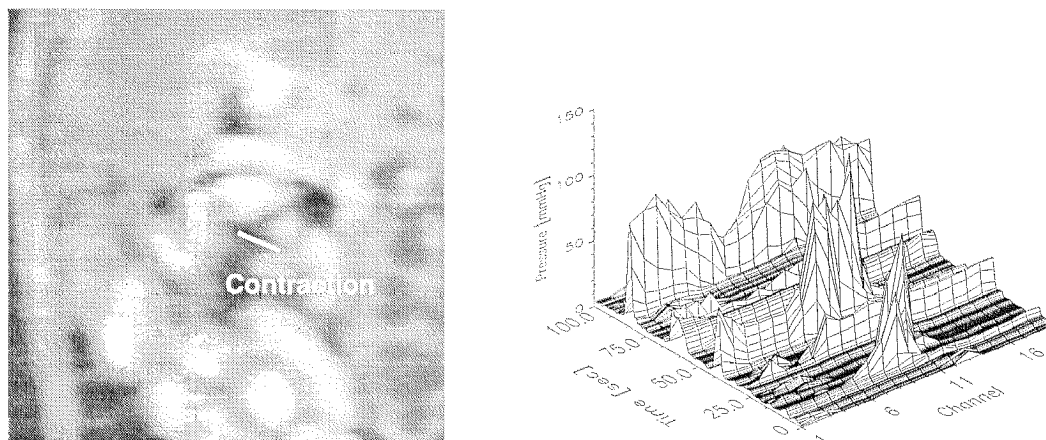

Figure 2: (A) Antroduodenal motility during intraduodenal lipid infusion: the MR image shows the antropyloroduodenal area and an antral contraction. The proximal marker and parts of the assembly are visible and allow identification of the position of the sidehole chain of the assembly. The 3D representation of the corresponding manometric tracings (right) shows a high pressure band that coincided well with the pyloric position. (B) Erythromycin induced episodes of strong antroduodenal contractions (note the different pressure ranges in the plots).

Manometric evaluation: Before erythromycin, the median antral pressure wave activity expressed as the AUC was 5939 mmHg s (249 - 15755 mmHg s) for the first 15 min and 2673 mmHg s (932 – 16659 mmHg s) for the second 15 min. Median frequency of pressure waves before erythromycin was 2.7 /min (0 – 3.4 /min) and 2.4 /min (0 – 3.6 /min).

Median wave speed was 4.0 mm/s (0 – 5.5 mm/s) and 3.1 (2.4 – 5.8 mm/s). All antral pressure waves were antegrade (total number of pressure waves = 51; number of pressure events defined in single channels = 254). The amplitude of pressure events was 12.5 ± 5.5 mmHg. After erythromycin, episodes of strong antroduodenal contractions were observed, but antral activity was highly variable between subjects. The AUC after erythromycin was 17562 mmHg . s (2222 – 325296 mmHg . s). Median frequency of pressure waves was 1.1 /min (0.2 – 3.3 /min); median wave speed was 5.1 mm/s (2.5 – 8.4 mm/s).
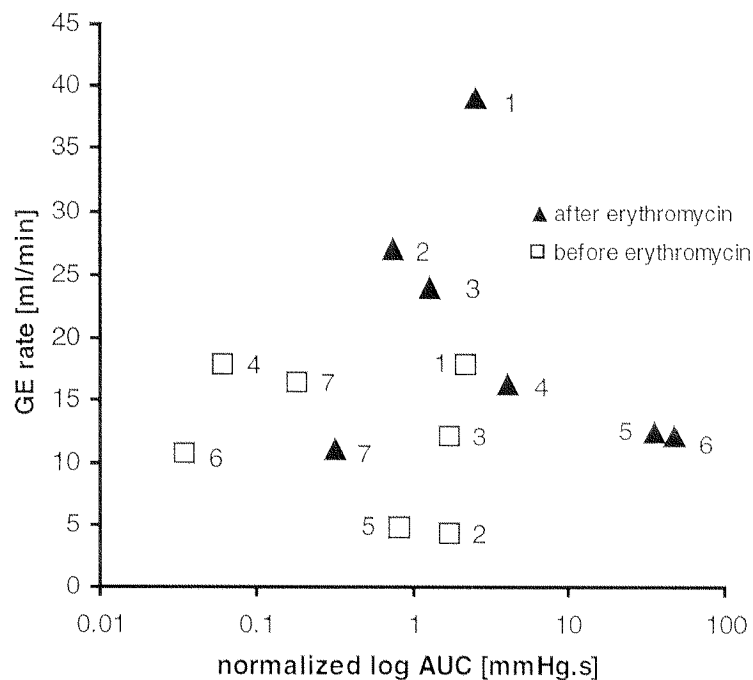

Figure 3: Emptying rate vs. AUC before erythromycin infusion, over 15 min after first gastric filling and after erythromycin infusion, over 15 min after second gastric filling. Antral activity could not be related to gastric emptying.

Comparison between manometric and MRI data: 82 % (51/62) of all observed contraction waves were detected manometrically. 49 % of all contractile events (241/496) were associated with a detectable pressure event. The degree of lumen occlusion of the contractile events that had no observed pressure change was 47 ± 15 %.

There was a tendency to an increased emptying rate after erythromycin, while antral contractile activity, expressed as AUC of antral pressure events, was not found to be different in the time period assessed after erythromycin (Figure 3). This was largely due to the delayed reaction of antral contractile activity to erythromycin infusion.

Prior to erythromycin, the pylorus appeared as a 6 - 9 mm thick structure separating antrum and duodenum and was observed to move forwards and backwards during antral contractions. The position of the pylorus as determined on the MR images coincided with a narrow (< 9 mm) zone of high pressure in the manometric recordings (pyloric pressure 7.8 ± 2.9 mmHg, antral pressure 3.7 ± 1.8 mmHg; duodenal pressure 3.2 ± 1.5 mmHg). The deviation of the MRI defined pylorus from the manometric port with maximum pyloric pressure over all subjects was 4.1 ± 0.6 mm, which corresponds to the magnitude of the MR image resolution (3·3 mm^2).

Discussion

In this work, high-resolution manometry and MRI were combined to assess the relationship between wall motion and pressure tracings during intragastric nutrient infusion.

During intraduodenal nutrient infusion, the anatomical pylorus corresponded to a high-pressure zone identified manometrically, which is consistent with the known stimulation of pyloric sphincter activity [8]. The lack of correlation between antral motor activity and gastric emptying during duodenal nutrient infusion may indicate that either antral contractions are not primarily responsible for gastric emptying in this situation, or that the commonly accepted parameters of antral motor activity (i.e. amplitude,

frequency, propagation speed of pressure waves, antral motility indices) are not the most relevant parameters [10]. In agreement with previous studies [3], we found that erythromycin altered the rate of gastric emptying and the pattern of contractile events in the antrum, leading to episodes of strong antral activity. Amplitudes of pressure events increased after erythromycin in all subjects, but there were large interindividual differences. While some subjects showed only a moderate increase and mostly peristaltic events, a distinct class of pressure events characterised by high amplitudes was prevalent in others. This probably reflects variations of individual susceptibility to erythromycin.

The study further aimed to investigate the relationship between wall motion and pressure tracings, especially in the situation of non lumen-occlusive contractions in the vicinity of the gastroduodenal junction. We acquired multiple slices in order to obtain three-dimensional information on anatomy and motility of the entire antroduodenal region. The pressure ports of the catheter were localised with the MRI markers on the assembly so that local pressure events could be related to local wall deformation in the antropyloroduodenal region. Thus uncertainty with the interpretation of manometric data due to movement of the assembly as a whole could be avoided, and we were able to discriminate between motion of the pylorus and the manometric catheter. We observed that manometry has a good sensitivity in detecting antral peristaltic contractions, while a substantial proportion of individual contractile events were not reflected in the pressure tracings. We did not find a simple relationship between the degree of lumen occlusion and pressure, which would provide a simple threshold for the ability of manometry to detect wall deformations. It is however reasonable to expect that pressure would be influenced by the propagation speed of the wave, the degree of lumen occlusion and, the geometry of the antrum and the contractile state of the pylorus.

Three-dimensional, dynamic information on wall motion obtained by MRI combined with pressure information from high resolution manometry provides novel insights into gastric mechanics and its modulation by nutrient stimulation and pharmacological agents. We have been able to correlate the contractile activity in the antrum with the associated pressure tracings. The lack of correlation between antral motor activity and

gastric emptying suggests that lumen-occlusive antral contractions are not primarily responsible for gastric emptying of non-nutrient liquid during intraduodenal nutrient infusion. Furthermore, erythromycin induced distinct changes in the pattern of wall motion of the distal stomach with the occurrence of strong contraction episodes.

References

1. Heddle R, Dent J, Read NW, Houghton LA, Toouli J, Horowitz M, Maddern GJ, Downtown J. Antropyloroduodenal motor responses to intraduodenal lipid infusion in healthy volunteers. Am J Physiol 1988;254:G671-679.

2. Janssens J, Peeters TL, Vantrappen G, Tack J, Urbain J L, De Roos M, Muls E, Bouillon R. Improvement of gastric emptying in diabetic gastroparesis by erythromycin. N Engl J Med 1990;322:1028-1031.

3. Fraser R, Shearer T, Fuller J, Horowitz M, Dent J. Intravenous erythromycin overcomes small intestinal feedback on antral, pyloric and duodenal motility. Gastroenterology 1992;103:114-119.

4. Horowitz M, Dent J, Fraser R, Sun W, Hebbard G. Role and integration of mechanisms controlling gastric emptying. Dig Dis Sci 1994;39:7-13.

5. Wright J, Evans D, Gowland P, Mansfield P. Validation of antroduodenal motility measurements made by echo-planar magnetic resonance imaging. Neurogastroenterol-Motil 1999;11:19-25.

6. Faas H, Kunz P, Hebbard G, Feinle C, Schwizer W, Fried M, Boesiger P. Combining ultra-fast 3D MR imaging and high resolution manometry to assess gastric motor function. Proceedings ISMRM 5th annual meeting1997:960.

7. Schwizer W, Fraser R, Borovicka J, Asal K, Crelier G, Kunz P, Boesiger P, Boesiger P, Fried M. Measurement of proximal and distal gastric motility with magnetic resonance imaging. Am J Physiol 1996;271:G217-G222.

8. Heddle R, Dent J, Toouli J, Read NW. Topography and measurement of pyloric pressure waves and tone in humans. Am J Physiol 1988;255:G490-497.

9. Kunz P, Crelier GR, Schwizer W, Borovicka J, Kreiss C, Fried M, Boesiger P. Gastric emptying and motility: assessment with MR imaging - preliminary observations. Radiology 1998;207(1):33-40.

10. Camilleri M, Malagelada JR, Brown ML, Becker G, Zinsmeister AR. Relation between antral motility and gastric emptying of solids and liquids in humans. Am J Physiol 1985;249:G580-5.

Chapter 3

Relative contributions of "pressure pump" and "peristaltic pump" to gastric function

[1] Indireshkumar K, [1] Brasseur JG, [2] Faas H, [3] Hebbard GS, [2] Kunz P, [3] Dent J, [4] Feinle C, [1] Li M, [2] Boesiger P, [4] Fried M, [4] Schwizer W.

[1] Bioengineering Division, Department of Mechanical Engineering, Pennsylvania State University, State College, Pennsylvania, USA, [2] Biophysics Division, Institute of Biomedical Engineering and Medical Informatics, University and ETH Zurich, [3] Royal Adelaide University Hospital, Adelaide, Australia, [4] Department of Gastroenterology, University Hospital Zurich, Switzerland

Abstract

The relative contributions to gastric emptying from common cavity antroduodenal pressure difference ("pressure pump") vs. propagating high pressure waves in the distal antrum ("peristaltic pump") were analyzed using time-resolved 3-D MRI concurrent with high resolution manometry during intraduodenal nutrient infusion at 2 kcal/min. Gastric volume and space-time pressure and contraction-wave histories in the antropyloroduodenal region were assessed in 7 healthy subjects. The subjects fell into distinct "high" (n = 4) and "low" (n = 3) antral pressure activity groups, where the high activity group had lower average rate of gastric emptying. Pressure history in the distal antrum was dominated by periods of relative quiescence and pressure during quiescence remained unchanged during emptying, suggesting that common cavity pressure levels were maintained by increasing wall muscle tone with decreasing volume. The aboral progression of antral high-pressure events was correlated with increasing pyloric resistance, indicating that transpyloric flow tended to be blocked during antral contraction-wave activity. We conclude that emptying, delayed by duodenogastric feedback, is dominated by the "pressure pump" mechanism controlled by pyloric opening during periods of relative quiescence in antral pressure- and contractile-wave activity.

Introduction

Although animal studies indicate that gastric emptying is often pulsatile and that the pylorus is important in regulating the rate of gastric emptying [1-4], the patterning of antral motor and pressure events, their coordination with pyloric opening and their relative contributions to gastric emptying in humans are not well understood. For example, intermittent transpyloric flow could, in principle, be created by either intermittent increases in antral pressure in the presence of a relatively constant pyloric resistance, or by intermittent pyloric opening in the presence of relatively constant antroduodenal pressure difference. In particular, the relative contributions of common cavity and phasic transpyloric pressure differences, the role of the pylorus in regulating transpyloric flow and the variations in these components with meal composition and volume have not been delineated [5, 6].

Mechanically, time-local components of gastric emptying may be grouped within "peristaltic pump" or "pressure pump" contributors to transpyloric flow. The "peristaltic pump" contribution to gastric emptying occurs during the short duration periods of pressure increase just proximal to the pyloric channel induced by an advancing contraction wave when the pylorus is open. The volume of transpyloric flow during these peristalsis-induced increases in P_A - P_D depends both on the magnitude and duration of phasic pressure increase and on the resistance to flow within the pyloric channel. Depending on the diameter of the pyloric channel, flow is directed both aborally and orally during phasic increases in antral pressure.

The "pressure pump" contributor to gastric emptying is associated with flow during periods of relative quiescence in contraction-induced pressure activity in the distal antrum. Like the peristaltic pump contribution, the rate of transpyloric flow depends on the magnitude of the common cavity pressure difference P_A - P_D and the resistance to flow, as determined by the diameter of the pyloric channel during the quiescent periods.

The relative contributions of peristaltic and pressure pump to gastric emptying depends on several factors, including the coordination between pyloric opening and phasic pressure excursions in the distal antrum, degree of and duration of opening of the pyloric channel during quiescent periods, and the magnitudes of antroduodenal pressure differences during pyloric opening periods. Furthermore, the combination of motor events responsible for emptying depends on physiological responses to the composition of the meal, to gastric volume and to pharmacological substances, which alter gastric or duodenal sensory function [5,7]. In this study we analyze local contributions to emptying delayed by controlled nutrient infusion in the proximal duodenum.

The aim of the present study is to assess the relative contributions to gastric emptying of the pressure and peristaltic pumps in humans during emptying of non-nutrient saline with the rate of emptying delayed by controlled intraduodenal nutrient infusion. To analyze these primary contributors to gastric emptying we have concurrently assessed intragastric pressure using high-resolution manometry [8] and antropyloroduodenal anatomy with 3-D MRI [9-12].

Methods

Subjects

Concurrent MRI and high-resolution manometry studies were performed on seven healthy subjects (five men, two women) age 23 to 45 years. All subjects gave written informed consent, and the study was approved by the Ethics Committee of the University Hospital Zurich.

Study protocol

Subjects fasted overnight prior to the study. The manometric assembly (4 mm outer diameter), and a second tube (2.5 mm diameter, used for intragastric instillation of saline) were passed into the stomach via an anesthetized nostril. The manometric assembly was positioned across the pylorus using transmucosal potential difference (see below). Following phase III of the interdigestive migrating motorcomplex, an intraduodenal infusion commenced. The infusion consisted of a nutrient liquid (equal volumes of 25% dextrose and 10% intralipid, 1.1 kcal/ml, Kabi-Vitrum, Stockholm, Sweden) delivered at the rate of 2 ml/min (2.1 kcal/min) for the remainder of the study. After 30 minutes of infusion, the subject was transferred to the MR scanner and positioned lying 30° to the right side to ensure filling of the antrum. An isotonic saline solution (750 ml volume) was then infused into the gastric lumen over about 4 minutes. The saline was marked with 600 µM Gd-DOTA (Laboratiore Guerbet, Aulnay-sous Bois, France) as a contrast agent for MRI. All MRI studies were performed using a Philips Gyroscan ACS-NT 1.5 Tesla whole body scanner.

All data evaluated were collected during the first part of the study. Within 2-3 minutes after the stomach was filled, a MR "volume scan" was performed to measure the volume of liquid in the stomach. Two additional volume scans were performed 15 and 30 minutes later in order to assess the rate of gastric emptying. Between each pair of volume scans, three "motility scans" were carried out to assess changes in antropyloroduodenal anatomy over time. Manometric pressures were recorded uninterrupted throughout the study with the exception of periodic short periods for recalibration of manometric reference pressure[11].

MR Imaging

Volume scans: To determine intragastric liquid volume, a Turbo Spinecho scan (TR = 576 msec, TE = 12 msec) with 24 contiguous slices (7.5 mm slice thickness) was performed over 60 s using a previously established methodology [13]. In-plane pixel resolution was 1.5 mm (256 · 256 pixels; field-of-view = 384 mm). To minimize motion artifacts the scan was divided into four periods of 15 seconds each and the subjects were asked to hold their breath during each period. The measured volume necessarily included both the ingested liquid and gastric secretion.

Motility scans: To assess antropyloroduodenal motility and pressure-geometry relationships, rapid multi-planar scans were carried out over multiple 90 s periods. Seven slices were imaged per second using a multislice gradient echo EPI sequence (coronal slice orientation; EPI factor 55; TE = 5 ms; TR = 81 ms; flip angle = 20°; matrix size = 128 · 128 pixels with a resolution of 3 mm; field-of-view = 384 mm; slice thickness = 7 mm). The scan was triggered by a signal from the computer controlling manometric data acquisition to synchronize MRI with manometry.

Manometry

A perfusion manometry system (Dentsleeve, Australia) with optimized electronics (transducer drift < 0.1 mmHg/15 min, Sedia, Fribourg, Switzerland) was used to record pressures along a catheter with 21 ports (0.4 mm lumen diameter, 4 mm outer diameter), 19 of which were used for pressure in this study and one for intraduodenal nutrient infusion. The catheter was preflushed with CO_2 to eliminate air bubbles and water perfusion was limited to 0.08 ml/min. To obtain high spatial resolution through the antropyloroduodenal region, the 19 pressure recording ports were spaced 3.3 mm apart along a 6 cm segment of the assembly. The third and seventeenth sideholes were perfused with normal saline from separate reservoirs and transmucosal potential difference (TMPD) was measured concurrent with manometry to aid the positioning of the catheter across the pylorus. To identify the position of the catheter on MR images, two small stainless steel markers were placed on the catheter at each end of the 19-hole array. The manometric data were recorded for the entire duration of the study at 8 samples/s. Transducer drift was regularly corrected over the study period using an

underwater reference and measurement uncertainty was minimized to within 0.5 mmHg [8]. The infusion port was roughly 14 cm below the pylorus.

Data analysis

The data analyzed were limited to times during which the TMPD readings indicated correct placement of the catheter across the pyloric channel [6]. Pressure data were analyzed using several statistical techniques as described below. In preliminary analysis it was determined that stable statistics for pressure differences required about 2000 samples collected at 8 samples/s (i.e., about 4 minutes of data).

Statistical analysis of pressure characteristics associated with transpyloric flow required accurate determination of the location of the pylorus along the catheter as a function of time. To this end, the manometric data were interpolated between ports using splines and plotted as contours of constant pressure ("isocontours"). During intraduodenal nutrient infusion a relatively well-defined band of high pressure was observed in the isocontour plots for all subjects, extending roughly 6 - 10 mm along the lumen.

Antral, pyloric and duodenal ports: We defined the "pyloric port" as the manometric port closest to the local maximum in pressure within the high pressure band. The proximal and distal extremities of the pyloric channel were subsequently identified by the "antral port" and "duodenal port" defined as the manometric ports 1cm proximal and 1cm distal from the pyloric port, respectively. Because the antral, pyloric and duodenal ports are defined relative to the space-time distribution in antropyloroduodenal pressure, the catheter sideholes, which define these ports, can change with time.

Table 1. Basal pressures P* and shoulder pressures (P_{SP}) using the entire manometric dataset. Pressures are given relative to P_D*.

Subject	P_A*	P_P*	P_{SP}-P_A*
S1	0.4	2.7	3.5
S2	2.8	3.8	3.5
S3	0.0	1.4	4.4
S4	0.4	2.2	3.3
S5	0.6	3.3	4.1
S6	1.1	2.6	4.0
S7	3.7	5.6	4.5

Basal Pressures: Antral, pyloric and duodenal basal pressures (P_A*, P_P* and P_D*) were defined as the average value of the lowest 5 % of the manometric pressures recorded in the antral, pyloric and duodenal ports, respectively, over the entire data period, excluding recalibration and TMPD misalignment periods. (As a check, P_A* was also calculated by including all antral channels. The difference between the two approaches was within the imprecision of the measurement.) Because gastric emptying is associated with antroduodenal pressure difference, all pressures were referenced to the duodenal basal pressure (P_D*) unless otherwise indicated. Pyloric and antral basal pressures are catalogued in Table 1.

Level of antral pressure activity: We quantify the differences in levels of phasic and nonphasic pressure activity between subjects in relationship to the existence of "high pressure events" (HPE), where a HPE is defined as a group of pressure values in any antral channel which exceed a predefined fixed threshold relative to antral basal pressure P_A*. That is, a HPE is a period where P - P_A* exceeds a predefined value P_{HP} - P_A*. Because these periods were used to compare between subjects, the threshold P_{HP} - P_A* was set to the same level for all subjects. We discuss below our basis for choosing

the particular HPE threshold, $P_{HP} - P_A^* = 5$ mmHg. Antral pressure activity in individual subjects was then quantified using the following statistical measures:

1. *Maximum Area Under Curve (MaxAUC)*. The area under curve (AUC) was defined in each antral channel as the area under the pressure vs. time curve during HPE periods. The AUC was calculated with P_A^* as the baseline and the result scaled to a total time period of 30 min. To account for intrasubject differences in pressure-wave positioning, the antral channel with the maximum area under curve (MaxAUC) was used to distinguish levels of antral pressure activity between subjects.

2. *Average Pressure of HPEs*. The "average pressure of high pressure events" was defined as the average pressure during HPE periods, relative to the antral basal pressure, in the channel with MaxAUC.

3. *Total duration of HPEs*. The "total duration of high pressure event periods" is the time (in seconds) over which HPEs occurred, scaled to 30 minutes, in the antral channel with MaxAUC. Thus, MaxAUC = (Average Pressure of HPEs) · (Total duration of HPEs). Further discussion of these quantifications is given in Table 2.

"Active" vs. "quiescent" periods and High Pressure Events: In order to contrast the relative contributions to gastric emptying of progressive antral pressure events (peristaltic pump) with the intermediate periods of relative quiescence (pressure pump), we first separated antral pressure-time history into subject-specific "high" and "low" pressure periods using the "shoulder" pressure, P_{SP}, as described in the Appendix. The definition of P_{SP} follows from the pressure-time history in the distal antrum in individual subjects which, as in Figure 2a, has the structure of spikes of high pressure activity rising from a bed of low level pressure fluctuations. As described in detail in the Appendix, P_{SP} is an objective measure of pressure, obtained from the "cumulative frequency distribution" (see Figure A1) that defines the transition between the lower-level pressure fluctuations and the higher, spikier pressure events in the antral pressure port.

Table 2: Volume of gastric emptying (VGE) and characteristics of antral HPEs during 30 min. periods. MaxAUC = maximum of $\Sigma(P_i - P_A^*) \Delta t$ for all samples $(P_i - P_A^*) > 5$ mmHg. Columns IV and V derive from channel with MaxAUC. Average pressure of HPEs (relative to $P_A^* = 1/N$ $\Sigma (P_i - P_A^*)$ for all samples $(P_i - P_A^*) > 5$ mmHg, where N is the total number of samples. Total duration of HPEs = (MaxAUC)/(Average pressure of HPEs). Frequency of propagating HPEs = number of HPEs per minute that propagate at a speed of 24 mm/s (determined from isocontour plots). "Low pressure gap" is an estimate of the low-pressure region between antral propagating HPEs and the pyloric channel in the "high pressure activity" group.

I	II	III	IV	V	VI	VII
Subject	VGE [ml]	MaxAUC [mmHg.s]	Average pressure of HPEs [mmHg]	Total duration of HPEs [s]	Frequency of propagating HPEs [/min]	Low pressure gap [cm $\pm$ SD]
S1	460	172	5.8	29.6	0.00	
S2	424	1623	11.7	138.7	1.10	1.4 $\pm$ 0.5
S3	408	272	6.4	42.5	0.00	
S4	356	60	8.0	7.5	0.00	
S5	290	1322	7.5	176.3	1.18	1.3 $\pm$ 0.5
S6	160	1598	9.6	166.5	0.63	3.1 $\pm$ 0.3
S7	130	1660	8.2	202.4	0.96	1.6 $\pm$ 0.6

As shown in Table 1, relative shoulder pressure, $P_{SP} - P_A^*$, was between 3.3 and 4.5 mmHg for all subjects (3.9 $\pm$ 0.43 SD). For this reason we chose the fixed threshold $P_{HP}-P_A^* = 5$ mmHg, a value just above the highest value of $P_{SP} - P_A^*$, to define "high pressure events" (HPEs) in all subjects (Stemper and Cooke[14] used the same threshold for counting HPEs in the antrum based purely on subjective observation). "Active" periods are therefore those periods within HPEs, that is when pressure $P_A - P_A^*$ exceeds 5 mmHg, whereas "quiescent" periods are those in between, where relative pressure is below 5 mmHg.

Propagating HPEs, nonpropagating HPEs and quiescent periods: We isolated HPEs for all antral channels on the computer, then compared the locations and structure of the extracted HPEs with corresponding space-time structure of pressure in the isocontour

plots. From this comparison we subjectively separated all HPEs into "propagating" and "nonpropagating" groups. As an objective criterion, we required that all propagating HPEs appear clearly on the isocontour representation as pressure waves with wave speed between 2 and 4 mm/s. Once the propagating subclass of HPEs was extracted, the remaining time periods were divided into "nonpropagating HPEs" and "quiescent periods". In this way, the pressure-time history in the antral ports of all subjects was subdivided into propagating HPEs (PHPE), nonpropagating HPEs (NPHPE) and quiescent periods (QP).

Window means: The time mean of quantity X (where X could be pressure, pressure gradient, etc.) was defined over specified periods excluding the periods where the TMPD readings indicated incorrect placement of the catheter across the pyloric channel. To assess the variation of basal and mean pressure with time, we divided the data period into shorter time intervals, or "windows", and computed the mean and basal pressures within each window. The minimum time interval had to be sufficiently long to contain enough sample for stable statistics. Tests suggested that at least 1000 pressure samples (at 8 samples/s) were required for stable statistics, so the total time interval was separated into three time windows with a minimum of 2000 pressure samples in each window. Basal pressure and time averages were computed for each time window.

The pressure gradient $\Delta p/L_p$ across the pyloric channel was estimated as $(P_A-P_D)/L_p$, where the length L_p is the distance between the antral and duodenal ports (2 cm).

Results

Emptying vs. high pressure activity in the antrum

In Table 2 subjects are numbered from the highest to the lowest gastric volumes emptied during the first 30 minutes (VGE). Note that the VGE differed widely among subjects and that the average pressure during HPEs varied from 5.7 to 12.0 mmHg above the antral basal pressure with no correlation with volume emptied. However, the max area under curve (MaxAUC) varied from 60 mmHg.s to 1660 mmHg.s in such a

way that all subjects could be separated into "high" and "low" antral pressure activity groups (Figure 1). Correspondingly, the total durations of HPEs were significantly higher in the high antral pressure activity group (Table 2). As indicated in Table 3, the low activity subjects displayed no propagating high pressure events, and a significantly higher percentage of time was occupied by quiescent periods (98 % ± 2.8 SD vs. 76 % ± 9.4 SD) in the low-activity group. Nevertheless, Figure 1 indicates that the average volume of liquid emptied was higher in the low pressure activity group (251 ml in the high activity group vs. 408 ml in the low activity group). The correlation coefficient between VGE and MaxAUC was - 0.65.

Whereas subjects in the low activity show relatively little high pressure activity proximal to the pyloric channel, those in the high activity group show clear high amplitude peristaltic pressure wave activity. These time-space pressure characteristics were typical of the two groups. Antral pressure waves terminated roughly 1 cm preceding the pyloric channel creating a gap of low pressure. The length of this "low pressure gap" is tabulated in Table 2 for the four "high activity" subjects. Subject 6 differed from the other three high activity subjects S2, S5, and S7 in that the low pressure gap was over twice as wide (3.1 cm for S6 vs. 1.4, 1.3, 1.6 cm for subjects 2, 5 and 7). This difference affects the statistics (discussed below).
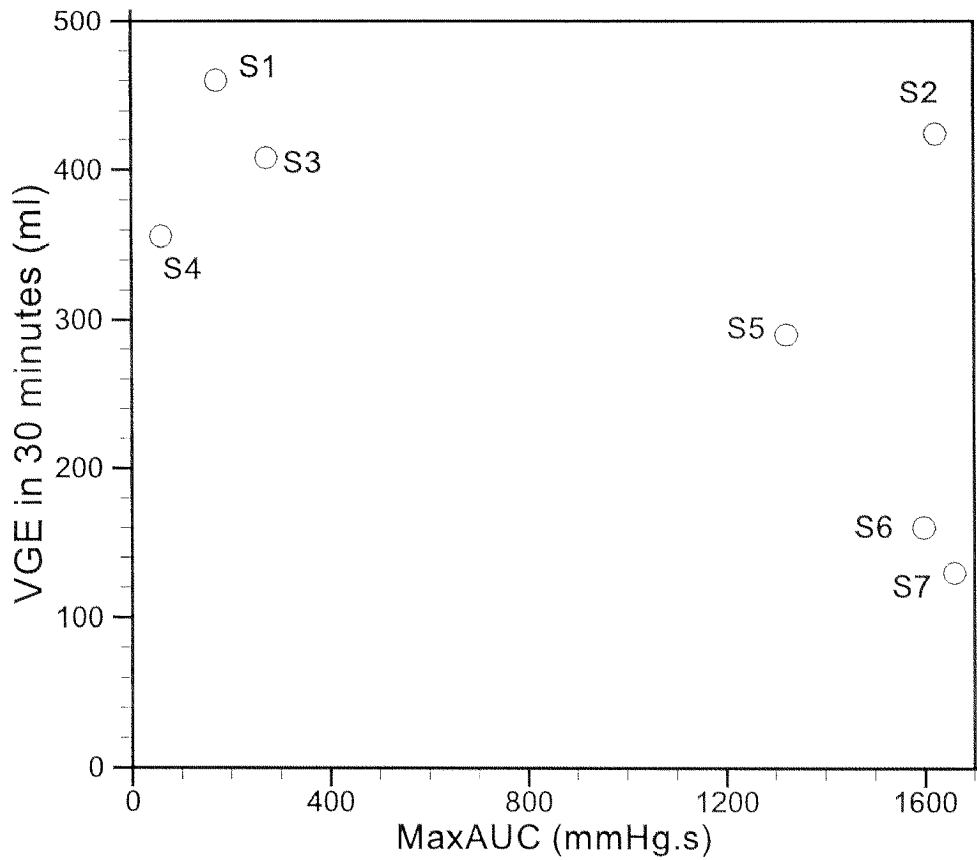
Figure 1: The level of antral pressure activity, as defined by MaxAUC, plotted against the volume of gastric emptying (VGE) over a 30 min. period between the first and third volume scans. The 7 subjects organized into "high pressure activity" (S2, S5, S6, and S7) and "low pressure activity" (S1, S3, and S4) groups. The average volume emptied in the high activity group (251 ml) was lower than the average VGE in the low activity group (408 ml).

Table 3: Percent of time occupied by quiescent periods (QP), Non Propagating High Pressure Events (NPHPE), and Propagating High Pressure Events (PHPE) averaged over the antral channels.

Subject	QP [%]	NPHPE [%]	PHPE [%]
S1	98.8	1.2	0
S2	73.4	3.3	23.3
S3	95.5	4.5	0
S4	99.8	0.2	0
S5	75.5	3.4	21.1
S6	89.8	3.1	7.1
S7	63.5	5	31.5

Basal and mean pressures, pressure gradient

Figure 2 show a representative example of time history of antral, pyloric and duodenal pressures measured from the antral port, pyloric port and duodenal port over approximately 30 minutes for "high activity" subject 2. All pressures are referenced to duodenal basal pressure. Particularly evident in antral and pyloric pressure are intermittent spikes in pressure overlying low-level pressure fluctuations. Also evident is the overall higher baseline pressure in the antrum as compared with the duodenum (see also Table 1). To assess the overall changes in background pressure during gastric emptying, we plot in Figure 3 average antral and pyloric port pressures measured within the "quiescent" periods in each of three time windows spanning the roughly 30-minute data periods (see Methods). Whereas "quiescent period" was defined in the antral port using the 5 mmHg threshold described in Methods, in the pyloric port the "quiescent periods" were defined using the shoulder pressure in that port (see Methods and Appendix). More importantly, there was no change in average pressure during the periods of quiescence during the 30 minute periods of gastric emptying ($p \approx 0.6$).
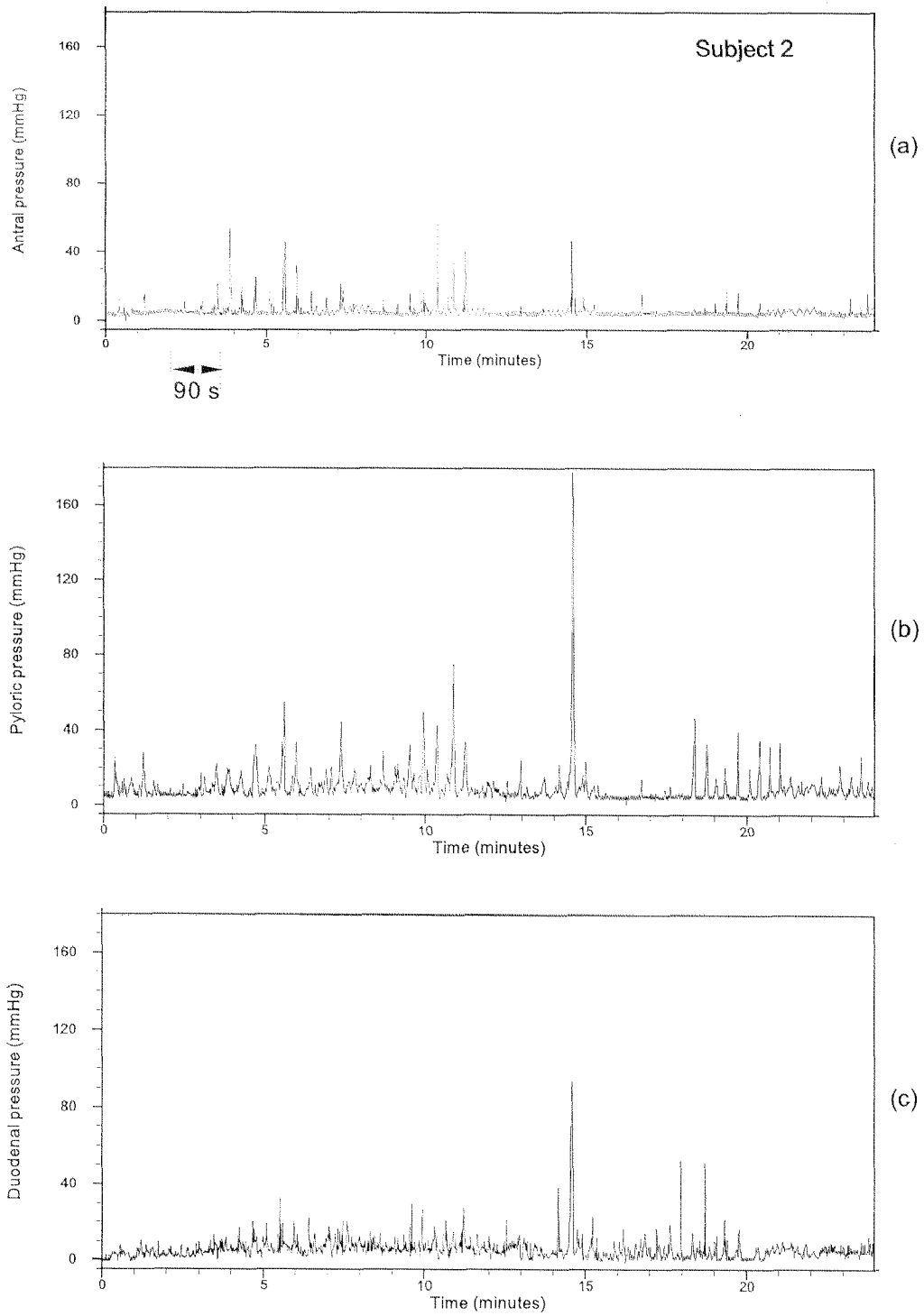
Figure 2: Example variations in antral, pyloric and duodenal pressures over roughly 30 min periods measured from the antral, pyloric and duodenal ports, respectively (see Methods) for subject 2 in the high antral pressure activity group (Figure 1).

In Figure 3, pressures are referenced to antral basal pressure, P_A^* (Table 1). Figure 3 indicates that the average pressure during quiescence in the pyloric channel is of order 2 mmHg above antral basal pressure.

Antropyloroduodenal pressure relationships

In Figure 4, the "active" and "quiescent" periods are shown in the pyloric channel and in the first three antral channels (see Figure 3 legend). The black bars identify "active" periods and the spaces between the black bars the "quiescent" periods in the given port. In the pyloric port the quiescent periods are those with the least pyloric resistance, and therefore the most likely to allow transpyloric flow. We observe that, during this 90 s period, the pyloric quiescent periods occur during periods of quiescence also in the antral channels, and that the resistance to transpyloric flow appears to be highest during antral pressure wave periods.

To determine if this observation is a general one, we search for a statistical relationship between antral peristaltic wave activity and pyloric resistance (measured by pressure) in the four high-activity group subjects. In Figure 5 we show pairs of frequency distributions for each subject of pressures in the pylorus during periods of propagating HPEs in the antrum (solid curves) and periods of antral quiescence (dashed curves), designated as described in Methods. Zero pressure on these plots is the duodenal basal pressure P_D^*; the vertical arrows indicate the pyloric basal pressure P_P^*.
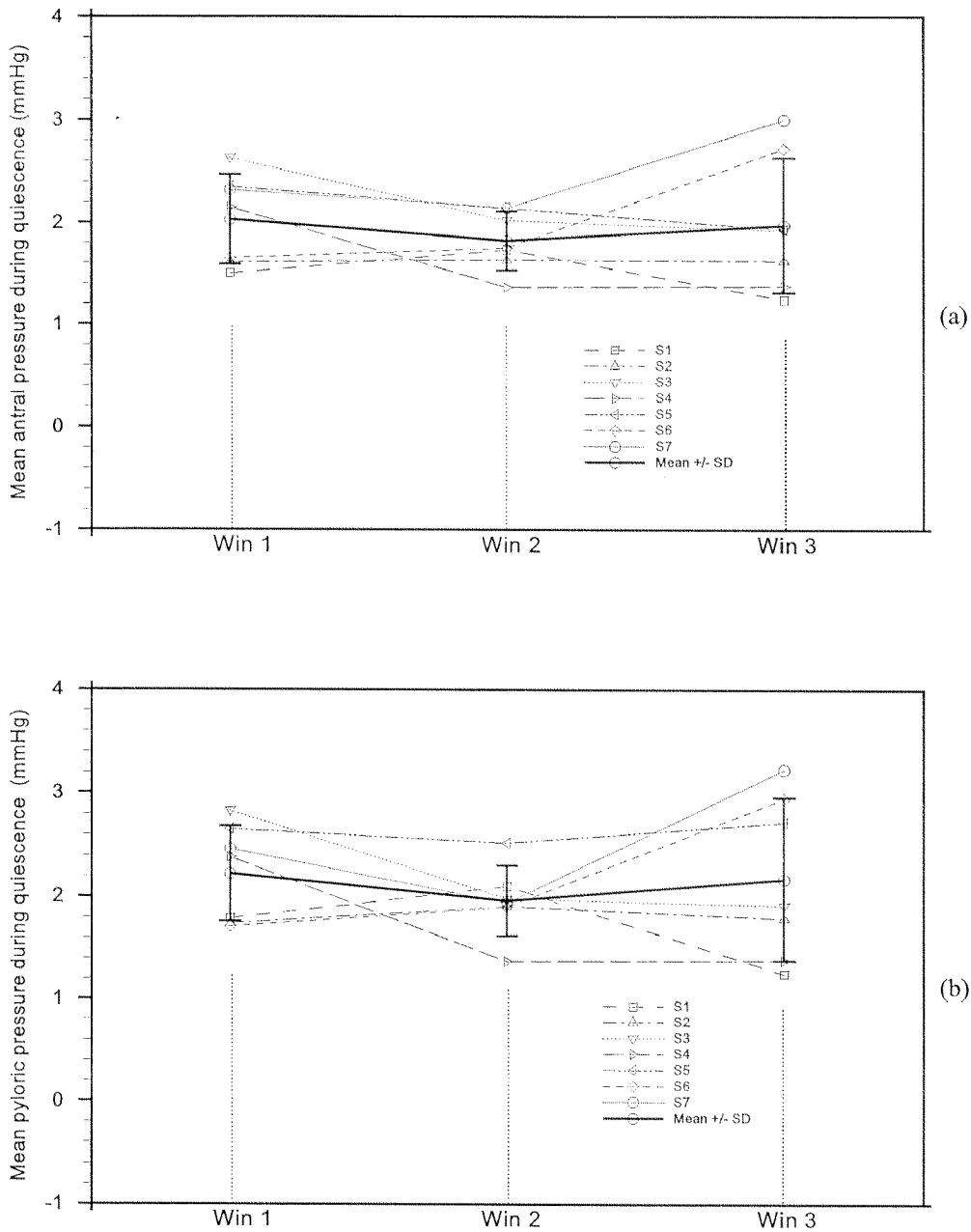
Figure 3: Average pressure statistics from the antral (a) and pyloric (b) ports over three time windows of 10 min each during periods "quiescent periods" of pressure variation in the respective ports. In the antral channel, "quiescence" is defined as the periods when pressure was below the HPE threshold $P_{HP} - P^*_A = 5$ mmHg. In the pyloric port "quiescence" is defined as periods when pressure was below the shoulder pressure P_{SP} obtained from the CFD of pyloric pressure (Appendix). All pressure statistics are given relative to antral basal pressure, P^*_A. The dark solid curves are averages over the seven subjects during each windowed period with standard deviation.
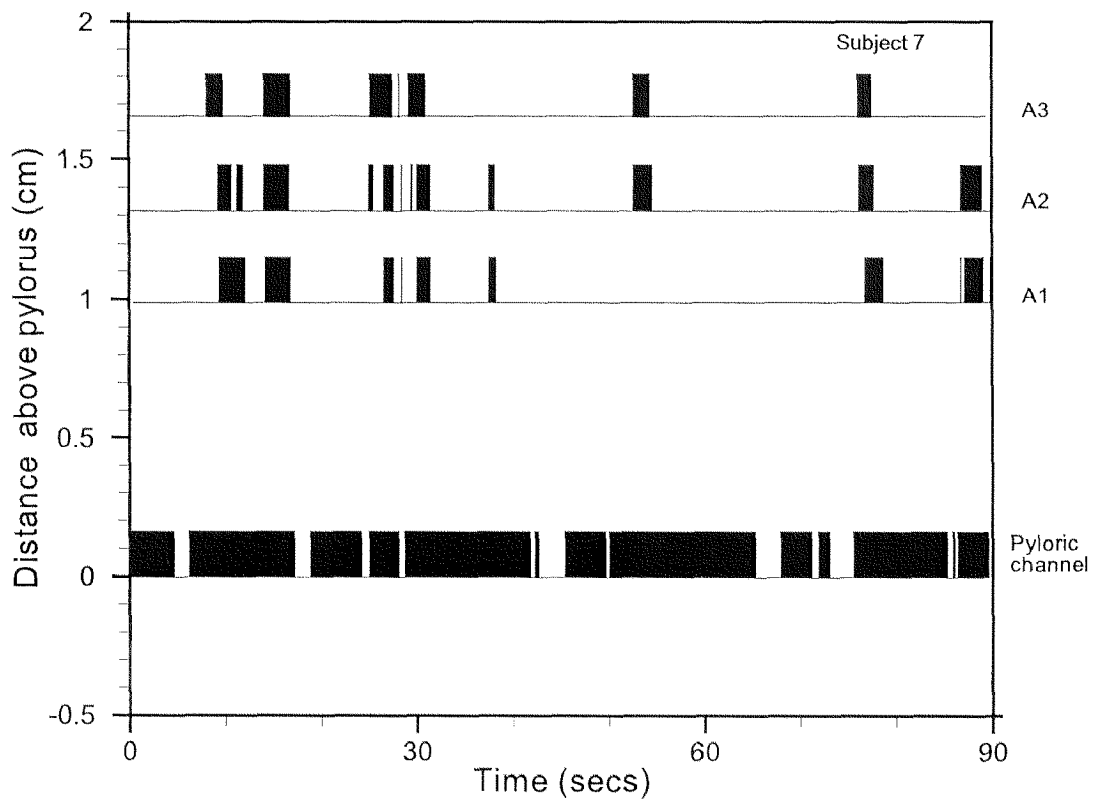
Figure 4: "Active" and "quiescent" periods in the pyloric channel and in the three antral channels over a 90 s time window. "Active" periods are shown with the black bars, and "quiescent" periods are those in between. In the pyloric channel "active" periods are those periods where antral pressure exceeds 5 mmHg relative to antral basal pressure. In the pyloric channel "active" periods are those where pressure exceeds the shoulder pressure defined for the pyloric channel from the CFD (Appendix). Note that the progressive antral pressure waves occur during periods when resistance to transpyloric flow is high, and that the quiescent periods in the pyloric channel tend to occur during quiescent periods in antral pressure.
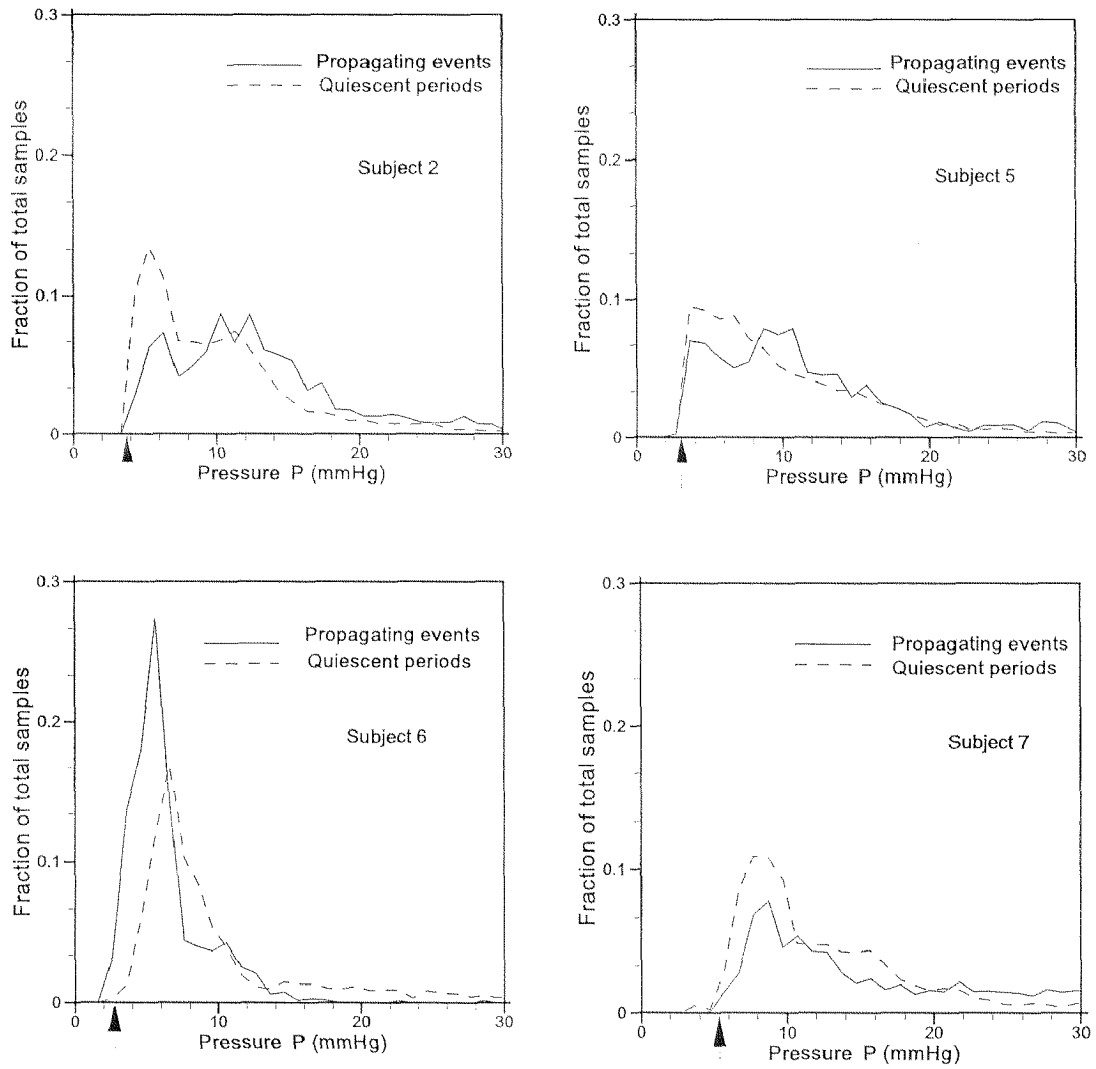
Figure 5: Fraction of total samples below a variable pressure P (Frequency Distribution), conditioned on periods of time where propagating HPEs exist in the antrum (solid curves) and on periods of quiescence in antral pressure activity (dashed curves) for the four subjects in the high activity group (Figure 1). Pressures are given relative to duodenal basal pressure P^*_D. The vertical arrows show pyloric basal pressure P_P^* (Table 1). In subjects 2, 5 and 7 the fraction of samples between P_P^* and P_P^* + 4 mmHg drops significantly during periods of antral propagating pressure waves. Such a drop does not exist in subject 6 due to the exceptionally large "low pressure gap" between the end of the antral contraction waves and the pyloric channel (Table 2).

Subjects 2, 5 and 7 display similar characteristics: at the lowest pyloric pressures, within a few mmHg from P_P^*, when the resistance to transpyloric flow is at a minimum, the fraction of samples during the existence of propagating antral HPEs is much lower than during quiescent period in the antrum. This drop in the fraction of pressure samples in the range P_P^* and P_P^* + 4 mmHg is roughly a factor of two and is statistically significant (p = 0.028). Thus, the probability of transpyloric flow, for these three subjects, is significantly higher during antral quiescent periods than during the existence of antral propagating pressure waves.

The same trend is not observed with subject 6. This difference is a direct reflection of the difference in extent of the "low pressure gap" which precedes the pyloric channel (see Figure 4b). Because the low pressure gap is over twice as wide in subject 6 as compared with subjects 2, 5, and 7 (Table 2), the antral peristaltic pressure waves progress to only within about 3 cm of the pyloric channel before terminating. As a consequence, these distant peristaltic pressure waves had little influence on pyloric pressure variation for this subject.

The relationship between pyloric resistance and antral pressure activity is analyzed further in Figure 6 where the level of pyloric resistance is correlated with the advancement of antral contraction waves. Specifically, average pyloric pressure for the periods when propagating HPEs pass each antral pressure port, is plotted in Figure 6 as a function of the antral port number. The antral ports are numbered A1-A8 from the most distal to the most proximal, each port separated by 3.3 mm beginning with port A1, which is 1 cm proximal to the pyloric port. The average pressure in the pyloric port is plotted relative to P_D^*.
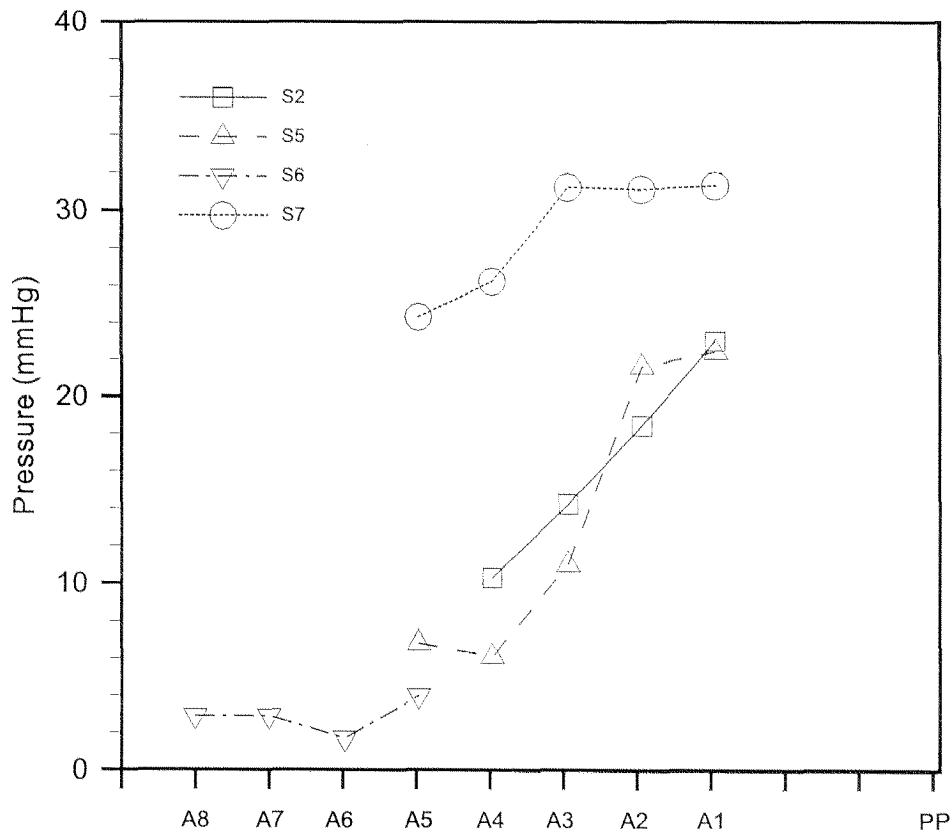
Figure 6: Average pressure at the pyloric port conditioned on the existence of propagating HPEs at different antral channels proximal to the pyloric port. A1-A8 on the lower axis indicate the location of the antral channels beginning with the "antral port" (1 cm above the pyloric port), and progressing proximally with each adjacent antral channel (each separated by 3.3 mm). The left axis indicates the average pressure in the pyloric port (relative to P^*_D during the periods when propagating HPEs could be found that the various antral ports, with A8 being the most distant port and A1 the closest to the pylorus. Pyloric pressure was higher when the pressure wave is closer to the pylorus.

Figure 6 shows that pyloric resistance increases as antral pressure waves move closer to the pylorus. The increase in pyloric pressure with decreasing distance from the pylorus is significant in subjects 2, 5 and 7 (p = 0.038). Consistent with Table 2, the advancing pressure waves in subject 6 terminate much more proximally than in subjects 2, 5 and 7. Figure 6 suggests that the pyloric response to the existence of antral pressure waves

may not begin until the antral waves are 2-3 cm above the pylorus and that the peristaltic pressure waves in subject 6 terminate before a pyloric response is triggered.

Discussion

Gastric emptying is analyzed in this study as a series of local transpyloric flow events which integrate to produce a reduction of gastric volume of 130 - 460 ml over a 30 min period (Table 2). Time-local transpyloric flow events can be classified in two groups: flow associated with local increases in antroduodenal pressure difference due to antrally propagating pressure waves, and flow associated with a common cavity pressure difference between the distal antrum and proximal duodenum in periods of quiescence between antral high pressure events. The first class of flow events may be identified mechanically as a "peristaltic pump" mechanism of flow and the second class as a "pressure pump" mechanism. Whereas it can be argued that propagating pressure waves originate from corresponding propagating contraction waves, common cavity pressure differences can arise from multiple tonic sources globally dispersed over the gastric wall.

On the other hand, flow can only occur in the presence of an open pylorus. The sensitivity of flow to degree of pyloric opening is evident through a relevant fluid-physics approximation for viscous flow through constrictions [15, 16]. From this model we learn that the rate of transpyloric flow at any instance in time is proportional to $(P_A - P_D)$ / RES, where $P_A - P_D$ is the antroduodenal pressure difference at given time and RES is pyloric resistance. RES is given by vis / D^4, where D is the average diameter of the pyloric channel and vis is the gastric fluid viscosity. Because the pyloric resistance is proportional to $1/D$ to the *fourth* power, there is great sensitivity between rate of transpyloric flow and pyloric diameter. Consequently, our evaluations of peristaltic vs. pressure pump contributions to gastric emptying center on correlations between antroduodenal pressure history and changes in pyloric resistance measured indirectly through pyloric pressure.

Gastric emptying follows from the relationships between the pressure forces, which move the gastric contents against frictional resistance and the gastric wall motions and muscle tone, which generate those pressure forces. To measure pressure-geometry relationships associated with emptying requires concurrent manometry with imaging in the antropyloroduodenal region where emptying is controlled, and where resolution requirements are most severe. We combined 3D MRI and high resolution manometry to monitor pressure-geometry motor events in the antropyloroduodenal regions of 7 subjects while simultaneously measuring changes in gastric volume over 15 min intervals during emptying of a nonnutrient liquid with intraduodenal nutrient infusion at 2kcal/min [11].

The seven subjects differed in the nature of high-pressure activity in the antrum; three subjects displayed little high-pressure activity and four subjects exhibited consistent propagating HP antral events. Consequently, the 7 subjects separated neatly into "high antral activity" and "low antral activity" groups quantified by area under curve (MaxAUC), frequency, and total duration of high-pressure events (HPE). Interestingly, the high activity group emptied, on average, at a lower rate than the low activity group (Table 2, Figure 2). This observation was the first indication that antral pressure wave activity may not play the dominant role in slowed gastric emptying.

A second indication was given by Figure 3, which shows that average antral pressure during quiescent periods of antral activity (and antral basal pressure) remained unchanged during reductions in gastric volume from 130-460 ml over 30 minutes. If the stomach wall were a purely elastic structure, emptying would imply decreasing elastic wall tension and decreasing intragastric pressure until the internal and external pressures equalize. Figure 3, on the other hand, suggests that active muscle wall tone increased, on average, during gastric emptying. Furthermore, whereas active tone apparently increased with decreasing gastric volume in all subjects, there was great variability in antral high-pressure activity among subjects (Table 2, Figure 1), suggesting that increases in active wall tone are independent of contractile activity within the antrum. Because transpyloric flow is driven by a positive pressure difference across an open pylorus, the maintenance of constant common cavity pressure levels in the presence of major reductions in gastric volume suggests a physiological response to

the decrease in gastric volume so as to maintain transpyloric flow in the absence of antral contraction-wave activity during periods of pyloric opening.

Furthermore, we found also that pyloric pressure during quiescent periods in the pyloric channel is insensitive to changes in gastric volume. Tougas et al. [17] found that increases and decreases in the pyloric pressure of order 2 mmHg relative to antral basal pressure appeared to be correlated with pyloric closure and opening, respectively. Thus, a significant decrease in the average pyloric pressure during quiescence over the 30-minute period might have suggested that gastric emptying was maintained by a continual increase in the duration of pyloric opening. By contrast, the insensitivity of quiescent pyloric and antral pressures to reductions in gastric volume suggest a significant role for common cavity pressure difference in gastric emptying.

Further evidence that the pressure pump contribution to gastric emptying during intraduodenal nutrient infusion may be significant is given in Table 3 where we find that antral pressure activity in the three "low activity" subjects (S1, S3, S4) is almost entirely "quiescent" with no evidence of antral propagating pressure waves. Surprisingly, the average rate of gastric emptying in these three subjects was higher than the four subjects which displayed high levels of gastric emptying (Figure 1), suggesting that the emptying was primarily from common cavity pressure difference in the presence of an open pylorus, and that antral peristaltic activity has the potential to impede emptying. For this to be the case transpyloric flow must be slowed during antral peristaltic pressure events. This conclusion follows from Figs. 4-6.

Figure 4 suggests that the presence of antral contraction waves is correlated with high pyloric resistance. Statistical evidence supporting this subjective observation is given in Figs. 5 and 6. For antral peristaltic contractions to contribute significantly to gastric emptying, increases in peristalsis-induced pressure in the distal antrum should be correlated with low pyloric resistance. We find just the opposite, however. Figure 5 shows that pyloric pressure was significantly higher during the presence of antral propagating pressure events than during quiescent periods of antral pressure activity, implying that the pylorus has a higher probability to be closed during the existence of peristaltic activity in the antrum than during the quiescent periods between high

46

pressure events. More significantly, Figure 6 suggests an interaction between pyloric resistance and location of advancing peristaltic pressure waves. Within a zone of influence, it appears that the closer is the peristaltic wave to the pylorus, the greater is the probability of the pylorus to be closed. The peristaltic waves in one "high activity" subject (S6) appear to terminate outside this zone of influence and pyloric resistance is not influenced by the advancing pressure wave (Figure 6). Because the antroduodenal pressure difference is unaffected by the propagating pressure waves in this subject, peristalsis does not contribute significantly to emptying.

We are lead to hypothesize, therefore, that when gastric emptying is sufficiently delayed by nutrient stimulation of the duodenum, antral peristaltic wave activity interacts with pyloric opening to increase pyloric resistance and impede transpyloric flow during local periods when the peristaltic events have the highest potential to contribute to gastric emptying. Furthermore, we hypothesize that this interaction occurs within a zone of influence which appears to be of order 2-3 cm from the pylorus. Clearly, additional study is needed.

We conclude from this study that during gastric emptying of liquids slowed by controlled duodenal nutrient infusion at 2 kcal/min, gastric emptying was dominated by "pressure pump" mechanics resulting from common cavity pressure differences between the distal antrum and proximal duodenum. Whereas antral peristalsis was common in 4 of the 7 subjects, the "peristaltic pump" mechanism of transport across the pyloric channel contributed only minimally to gastric emptying due to relatively refined physiological coordination between antral peristalsis and pyloric resistance. It should be stressed that these conclusions are for slowed gastric emptying with controlled intraduodenal infusion at 2 kcal/min. It would be of great interest to extend the analysis to a wider range of gastric emptying states.

Appendix

Cumulative Frequency Distribution and Shoulder Pressure

The antral port Cumulative Frequency Distribution (CFD) of pressure is shown in Figure A1 for subject 5 (with pressure characteristics similar to Figure 2a). The CFD is defined as the fraction of pressure samples below a variable pressure P plotted against P relative to the antral basal pressure P^*_A. Clearly the CFD must be 0 at P below the lowest pressure (approximately P^*_A), and the CFD must approach 1 as P approaches the highest pressure in the dataset. The shape of the curve between 0 and 1, however, is due to the structure of the signal. Figure 2a displays intermittent spikes in pressure rising from a low-level bed of pressure fluctuations. Consequently, as the threshold P increases from the basal pressure (P = 0), it encounters the highest density of pressure samples and the CFD increases rapidly (curve portion C in Figure A1). However, the density of intermittent spikes is much lower, so that as P increases from the lower-level fluctuations to the higher-level intermittent spikes the rate of increase in the CFD slows dramatically (B) and the CFD approaches a plateau (A) at the highest level spikes in pressure.

The pressures in the curve portion B represent the transition between high-pressure events and periods of relative quiescent. To objectively quantify a single pressure value that defines this transition, we identify the intersection pressure between two straight lines which are fit to curve segments A and C of the CFD, as shown in Figure A1. We term this transitional pressure the "shoulder pressure", P_{SP}.
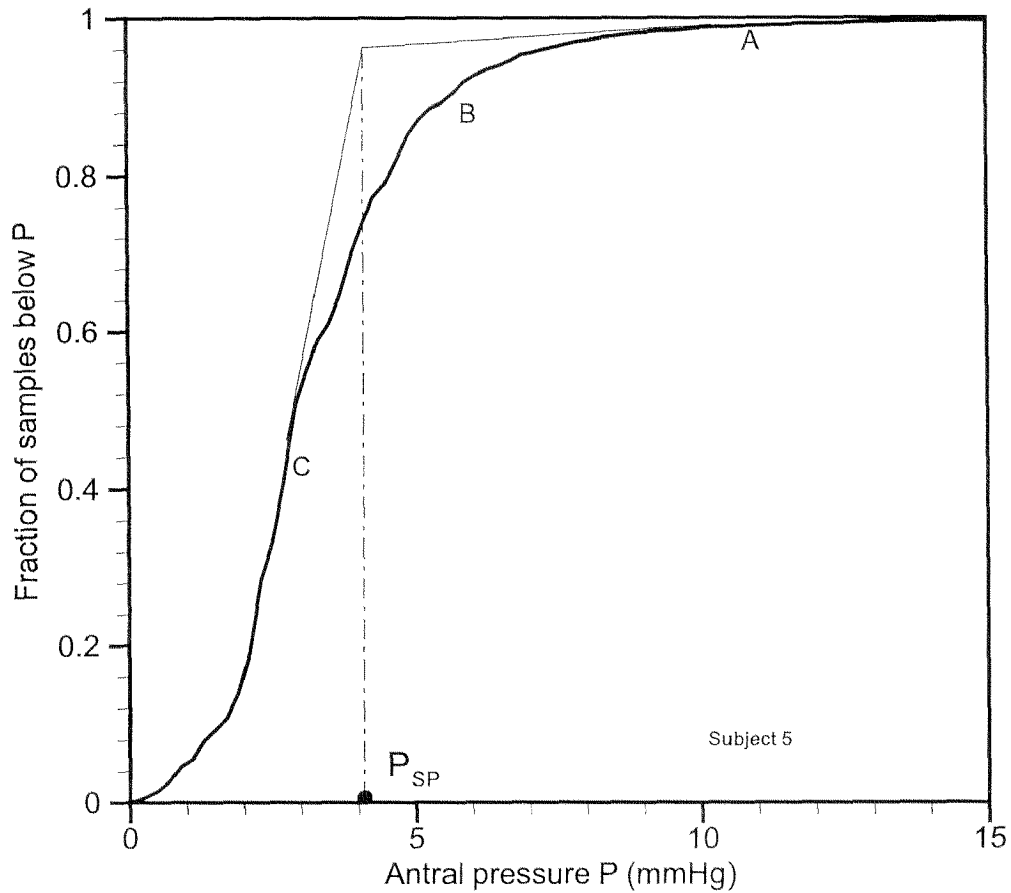
Figure A1: An example cumulative frequency distribution (CFD) from subject 5. The CFD is defined as the fraction of samples below a variable threshold P, referenced to antral basal pressure P^*_A, and was used to define a subject dependent "shoulder pressure" P_{SP} which demarcates the transition between lower level fluctuations and higher level spikes in the antral pressure time history (see Figure 2a).

References

1. Anvari, M., J. Dent, and G. G. Jamieson. Mechanics of pulsatile transpyloric flow in the pig. J Physiol 1995;488:193-202.

2. Malbert, C. H., C. Mathis, and J. P. Laplace. Vagal control of pyloric resistance. Am J Physiol 1995;269:G558-G569.

3. Treacy, P. J., G. G. Jamieson, and J. Dent. The importance of the pylorus as a regulator of solid and liquid emptying from the stomach. J Gastroenterology and Hepatology 1995;10:639-645.

4. Treacy, P. J., G. G. Jamieson, and J. Dent. Pyloric motor function during emptying of a liquid meal from the stomach in the conscious pig. J Physiol 1990;422:523-538.

5. Camilleri, M., J.-R. Malagelada, M. L. Brown, G. Becker, and A. R. Zinsmeister. Relation between antral motility and gastric emptying of solids and liquids in humans. Am J Physiol 1985;249:G580-G585.

6. Heddle, R., J. Dent, J. Toouli, and N. W. Read. Topography and measurement of pyloric pressure waves and tone in humans. Am J Physiol 1988;255: G490-G497.

7. Horowitz, M., J. Dent., R. Fraser, W. Sun, and G. Hebbard. Role and integration of mechanisms controlling gastric emptying. Dig Dis Sci 199439:7S-13S.

8. Hebbard, GS., H. Faas, C. Feinle, P. Kunz, H. Faas, P. Boesiger, M. Fried, and W. Schwizer. Technical aspects of high resolution perfusion manometry - An underwater zero improves accuracy of measurement of catheter offset and transducer drift (abstract). Gastroenterology 1997;112:A744.

9. Schwizer, W., H. Maecke, and M. Fried.Measurement of gastric emptying by magnetic resonance imaging in humans. Gastroenterology 1992;103:369-376.

10. Schwizer, W, R. Fraser, J. Borovicka, K. Asal, G. Crelier, P. Boesiger, J. J. Convers, A. L. Blum, and M. Fried. Effect of a calorie load on proximal and distal gastric motility measured by magnetic resonance imaging in humans. Gastroenterology 1993;104:A579.

11. Faas, H., G. Hebbard, P. Kunz, J. G. Brasseur, W. Schwizer, K. Indireshkumar, C Feinle, J. Dent, M. Fried, and P. Boesiger.Erythromycin induced alterations to antro-pyloro-duodenal motility studied by combined manometry and MRI (abstract). Gastroenterology 1998;114:A750.

12. Indireshkumar, K., J. G. Brasseur, H. Faas, G.S. Hebbard, P. Kunz, J. Dent, P. Boesiger, C. Feinle, M. Fried, M. Li, W. Schwizer. Variables affecting the difference in rate of gastric emptying among subjects (abstract). Gastroenterology 1998;114:A750.

13. Schwizer, W., R. Fraser, J. Borovicka, K. Asal, G. Crelier, P. Kunz, P. Boesiger, and M. Fried. Measurement of proximal and distal gastric motility with magnetic resonance imaging. Am J Physiol 1996;271:G217-G222.

14. Stemper, T. J. and A. R. Cooke. Gastric emptying and its relation to antral contractile activity. Gastroenterology 1975:69:649-653.

15. Brasseur, J. G. and W. J. Dodds Interpretation of intraluminal manometric measurements in terms of swallowing mechanics. Dysphagia 1991;6:100-119.

16. Li, M., J. G. Brasseur, and W. J. Dodds. Analysis of normal and abnormal esophageal transport using computer simulations. Am J Physiol 1994;266:G525-G543.

17. Tougas, G., M. Anvari, J. Dent, S. Somers, D. Richards, and G. W. Stevenson. Relation of pyloric motility to pyloric opening and closing in healthy subjects. Gut 1992;33:466-471.

Chapter 4

Visual vestibular conflict – Central modulation of gastric motor activity

Faas H, Feinle C, Boesiger P

Biophysics Division, Institute of Biomedical Engineering and Medical Informatics, University and ETH Zurich

Abstract

Input from the central nervous system plays an important role in modulating gastrointestinal function. The aim of the present study was to investigate the peripheral effects of a centrally acting stimulus, illusory self-motion (vection) on gastric motor function. Antral contractile activity and gastric volume retained after ingestion of a liquid meal was followed in twelve healthy subjects by magnetic resonance imaging. Vection was induced by an optokinetic drum following three different paradigms: (1) control situation: rest - rest; (2) vection – rest; (3) rest - vection – rest (rest = no rotation; vection: constant rotation of the drum). At regular intervals, subjects reported symptoms of illusory self-motion and nausea. Drum rotation induced the illusion of self-motion in all subjects and nausea in 11/12 subjects. Vection delayed gastric emptying (95 ± 4 % of volume retained at 28 min; control situation: 72 ± 4 %). Contractile strength was lower during vection than during the subsequent rest period (change in lumen occlusion: 25 ± 6 %, p < 0.05). Contraction frequency was also lower during vection (2.2 ± 0.3 /min) compared with the same period in the control situation (2.9 ± 0.2 /min; p < 0.05). The severity of nausea was not related to the inhibition of gastric emptying or changes in contractile activity. Vection inhibits antral contractile activity and slows gastric emptying independently of subjective symptoms reported. The present study takes advantage of the possibility to directly observe antral contractile activity by magnetic resonance imaging (MRI) as immediate and objective parameter to assess peripheral correlates of vection.

Introduction

The role that the brain exerts in the control of gastric function has been appreciated since the beginning of the century, when it was shown that emotional states evoked by external stimuli can have a profound impact on motor patterns in the GI tract [1,2]. Since then, a variety of environmental stimuli such as cold pressor stress, labyrinthine stimulation and motion stimuli have been demonstrated to affect gastric motility [3-5].

Vection has been used to investigate the effect of illusory self-motion on gastric function and to understand the nature of the accompanying physiological symptoms of motion sickness. Vection induces gastric rhythm disturbances determined by electrogastrography (EGG) [6,7] and slows gastric emptying [8]. However, gastric emptying is an integrated response to a change in overall gastroduodenal motor function. Therefore, its assessment does not allow more detailed conclusions, particularly on the timing and kinetics of the change with respect to the stimulus. Gastric pacemaker activity measured by EGG does not directly translate into contractile activity. The EGG reflects both electrical control activity, playing a permissive role for gastric contractions, and electrical response activity, reflecting the contractions themselves. As an outcome measure, antral contractile activity represents a directly assessable and immediate parameter. Changes in gastric emptying are a secondary effect, resulting from a complex interplay between different motor units. So far, no direct observation of gastric contractile activity during experience of vection has been reported.

The aim of our study was to directly assess the changes in gastric smooth muscle activity by magnetic resonance imaging (MRI) and relate them to symptoms of motion sickness during illusory self-motion.

Methods

Subjects

12 healthy subjects (4 male, 8 female) between 23 and 50 years (median 25 years) participated in the study. The subjects were not taking any medication and had no history of gastrointestinal disease. Written informed consent was obtained and the protocol was approved by the ethics committee of the University Hospital Zurich.

Study design

The study consisted of two parts: In part 1, the general effect of the vection stimulus in a horizontally oriented optokinetic drum (Figure 1a) on gastric emptying, motility and

symptoms was investigated (12 subjects). In part 2, the focus was on determining the kinetics of the changes in gastric smooth muscle activity under vection (2 subjects).
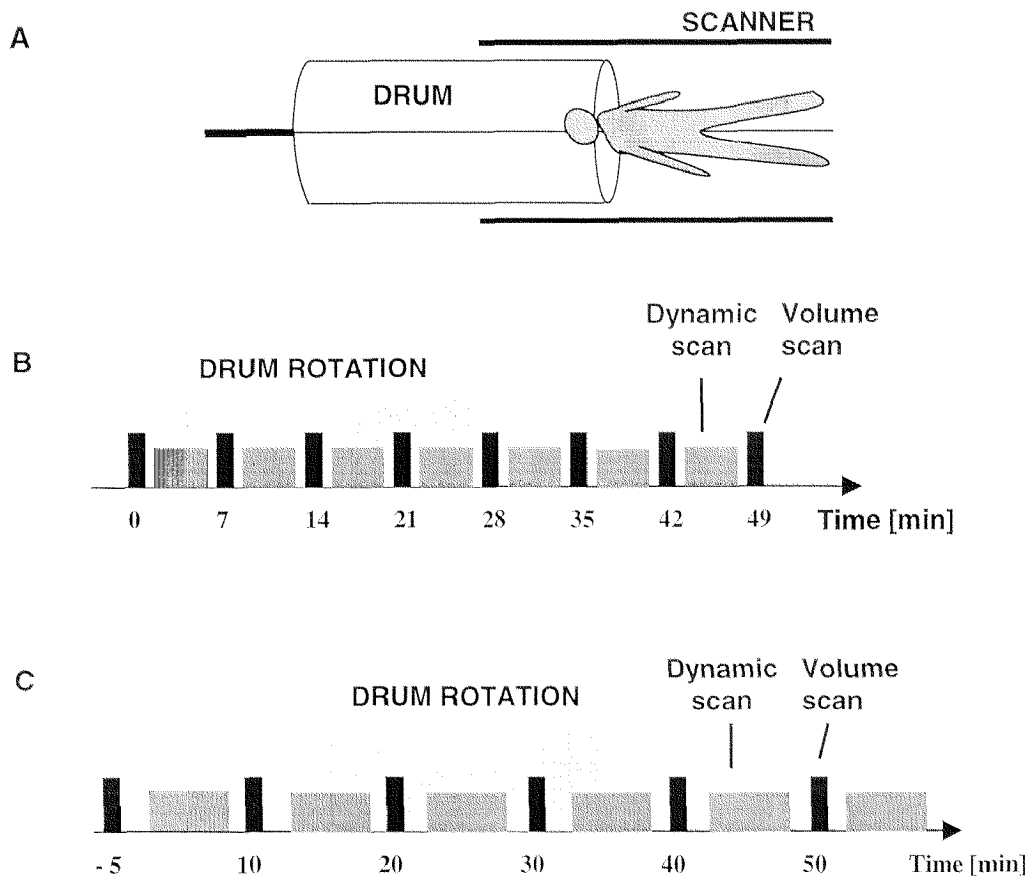

Figure 1: (A) The horizontally rotating optokinetic drum in the MR environment. (B) The protocol for study part 1 and (C) part 2.

Subjects attended the laboratory after fasting for at least 4 hours. After ingestion of 600 ml 15 % glucose solution, to which 600 µmol Gd-DOTA (Dotarem®, Laboratoire Guerbet, Aulnay-sous Bois, France) had been added as MR contrast agent, subjects were placed in the MR imager in a supine, 30° right angulated position, and a survey scan was performed. The subjects were positioned such that their entire visual field was covered by the inside of a horizontal optokinetic drum.

Vection drum

Illusory self-motion was induced by means of a circular vection drum (height: 1 m, diameter: 40 cm) made of MR compatible material and built by modifying a design

described previously [9] (Figure 1a). Alternating 5.7° black and 9.3° white vertical stripes covered the inner surface. The drum incorporated a transparent upper end to illuminate the inside of the cylinder and to allow observation of the subjects. The lid was connected via a shaft to an external motor which rotated the drum in anti-clockwise direction at a speed of 60 °/s. The drum was constructed such that its rotation axis was turned by 90° from an upright position and therefore could rotate around subjects in supine position in the MR imager. The subjects were positioned on a padded board in the scanner with their heads and shoulders resting on an extension reaching into the interior of the drum such that the drum ended at shoulder level. The subjects' faces were aligned with the rotation centre of the drum and their entire field of vision was covered by the drum and hence, the stripes.

MR Imaging

Volume scan: Intragastric liquid volume was assessed with a previously described method [10,11]. Briefly, a Turbo Spin Echo scan (transverse slice orientation, echo time TE = 12 ms, repetition time TR = 576 ms, flip angle 90°) with 20 contiguous slices (slice thickness: 10 mm) was performed over 60 s. The in-plane resolution was 1.5 mm (matrix size: 256 x 256 pixels, field of view: 380 mm). Scans were divided into four measurement periods of 15 s each, and the subjects were asked to hold their breath during the length of each of these measurements to avoid motion artefacts. Lipid signal suppression was achieved by selective excitation and gradient dephasing prior to the imaging sequence.

Dynamic scan: Using the thus obtained scan planes, dynamic high resolution images were acquired over 120 s (part 1) and 240 s (part 2) with a gradient echo sequence (T_R = 7.0 ms, T_E = 2.5 ms, α = 20°, in-plane resolution of 2 mm) to assess antral contractile activity with a time resolution of 1 s per image. The subjects were asked to breathe shallowly during image acquisition.

Assessment of symptoms

Immediately prior to each volume scan, subjects were questioned about their experience of symptoms of illusory self motion and nausea and asked to rate their

56

intensity on a scale from 0 to 10, with 0 indicating 'symptom not present' and 10 indicating 'symptom most severe'. In addition, during part 2 of the study, a modified version of the 'nausea profile'[12] was administered during baseline, during the drum rotation period and during recovery to assess cognitive-psychological (feeling nervous, afraid), central – physiological (feeling fatigue, weak, hot) and GI – peripheral physiological symptoms (feeling sick, stomach awareness).

Study protocol

Part 1: 12 subjects were studied on two occasions following the protocol in Figure 1b (vection – rest). 15 min after ingestion of 600 ml 15 % glucose solution, a first volume scan was performed (t = 0 min) to determine the initial amount of liquid in the stomach. This scan was repeated every 7 min until the end of the study period at 49 min. Following the volume scans, the contractile activity of the antrum was assessed using dynamic scans. On the first occasion, the drum was not rotated over the entire study period. On the second occasion, the drum was rotated from the first volume scan at 0 min until 28 min. Prior to each volume scan (i.e. every 7 min), the subjects were asked about the presence of symptoms and rated their intensity.

Part 2: On a separate occasion, 2 subjects were studied following the protocol shown in Figure 1c (rest – vection – rest). Subjects ingested 600 ml 15 % glucose solution. After a 20 min baseline period with no drum rotation, vection was induced over 20 min. After removal of the stimulus, the study was continued for a further 25 min.

Data analysis

Volume scan: In all 20 slices of each volume scan, the contour of gastric content was identified and outlined by a semi-automated edge detection algorithm. These areas were multiplied by the slice thickness and added to obtain momentary intragastric volume. Gastric emptying profiles were then constructed from gastric volumes by fitting the data to a power exponential model. A lag time was defined as the time up to which 90 % of intragastric content were retained.

Dynamic scan: From the dynamic MR scans, antral contractions were extracted and characterised by frequency and degree of lumen occlusion. The degree of occlusion of the gastric lumen by a contraction was measured manually and defined as the smallest distance between opposite sides of the gastric wall in the contracted state vs. the uncontracted state and expressed as percentage of lumen occlusion.

Statistical analysis

Data are expressed as means ± SEM. A paired, two tailed t-test was used to test for statistical significance. $P < 0.05$ was regarded as statistically significant.

Results

Part 1: vection (vection – rest) vs. control (rest – rest)

Symptoms

Illusory self-motion was experienced with moderate intensity by all subjects under vection ending when the stimulus was removed (Figure 2a). Subjects differed widely in the intensity of nausea ranging from no symptoms reported during the entire period to intense nausea (maximum score = 9; Figure 2b), which led in one case to early withdrawal of the stimulus.
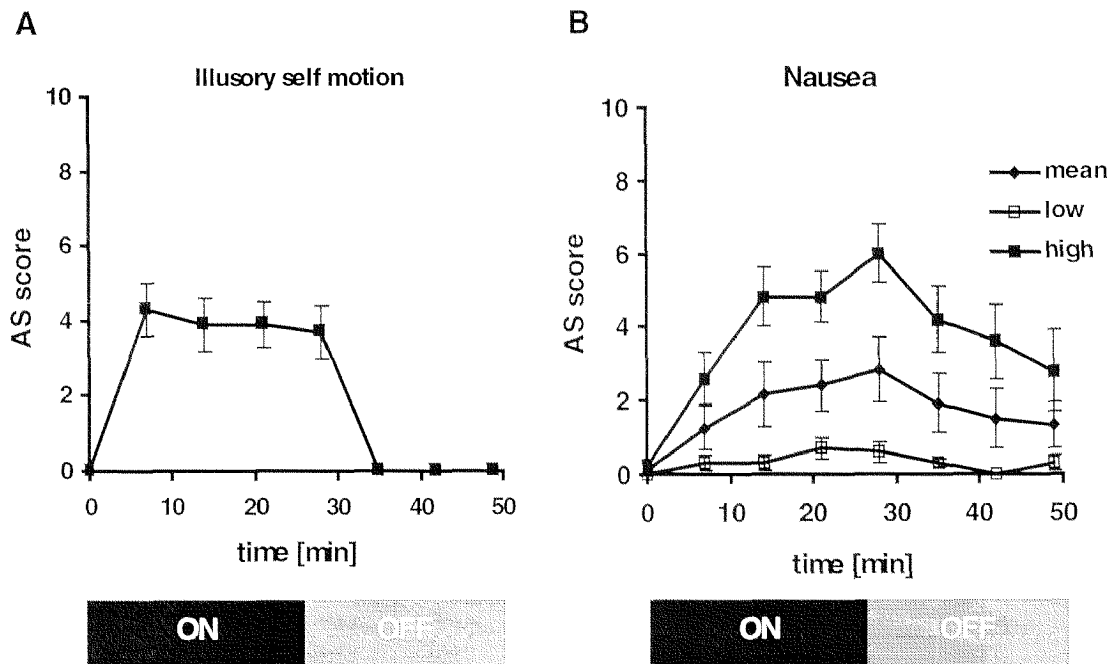
Figure 2: Illusory self motion (A) and nausea (B) as rated by the subjects on an analogue scale in study part 1. Self motion was perceived by all subjects under vection (ON) and disappeared upon withdrawal of the stimulus (OFF). Subjects fell in two groups with respect to their rating of nausea, high (n = 5) and low (n = 7).

Gastric emptying

Without the vection stimulus, gastric emptying followed a curvilinear pattern. Vection significantly delayed gastric emptying in 11 subjects, with 95 ± 4 % of volume retained in the stomach at 28 min (end of stimulus), compared with 72 ± 4 % in the control situation (lag time 33 ± 5 min compared with 10 ± 3 min in the control situation, Figure 3). The severity of nausea and inhibition of gastric emptying could not be related (linear fit r^2 = 0.03). One subject had faster emptying under vection (70 % of volume retained in the stomach at 35 min) than during control (100 % at 28 min).
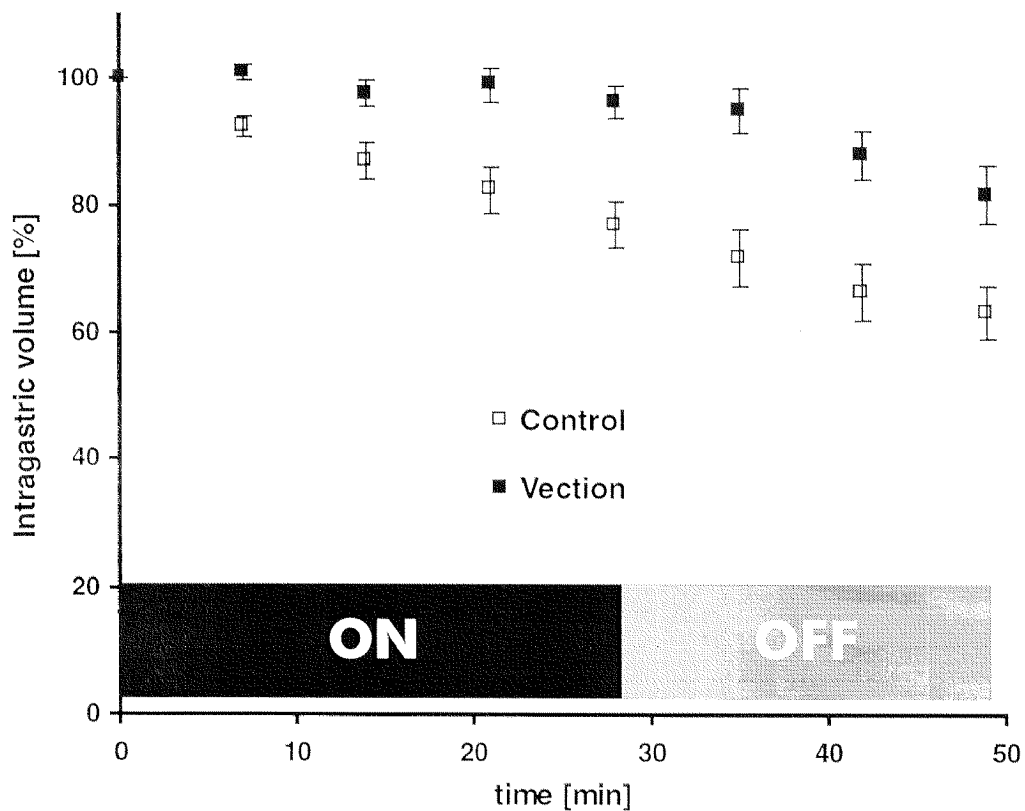
Figure 3: Gastric emptying was significantly delayed under vection as compared with control.

Contractile activity

A significant increase in lumen occlusion of the contractions (25 $\pm$ 6 %, p < 0.05, Figure 4) was observed between the vection and rest period, while no difference was found between the two periods in the control condition (change in contractile strength - 11 $\pm$ 11 %)). The severity of nausea and the contractile strength could not be related (linear fit r^2 = 0.16). During the stimulus, contraction frequency was lower (2.2 $\pm$ 0.3 /min) compared with the same period in the control situation (2.9 $\pm$ 0.2 /min; p < 0.05). After vection, frequency was 2.3 $\pm$ 0.3 /min compared with 2.9 $\pm$ 0.1 during control (p = n.s.).
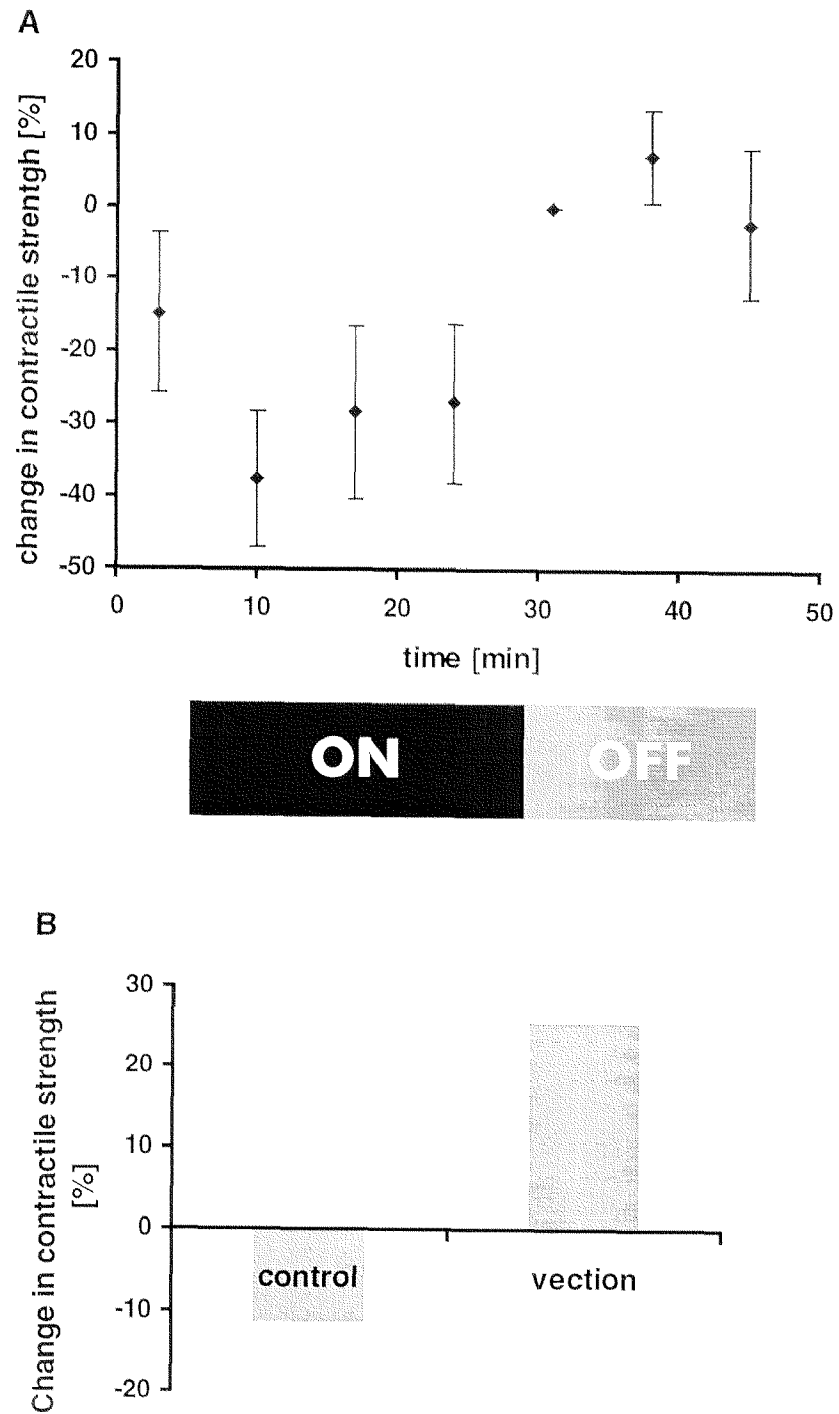
Figure 4: (A) Time course of the change in contractile strength during study part 1 (vection – rest), relative to the contractile strength after termination of the stimulus. (B) Differences in contractile strength between the vection (ON) and rest condition (OFF) and the control (rest – rest).
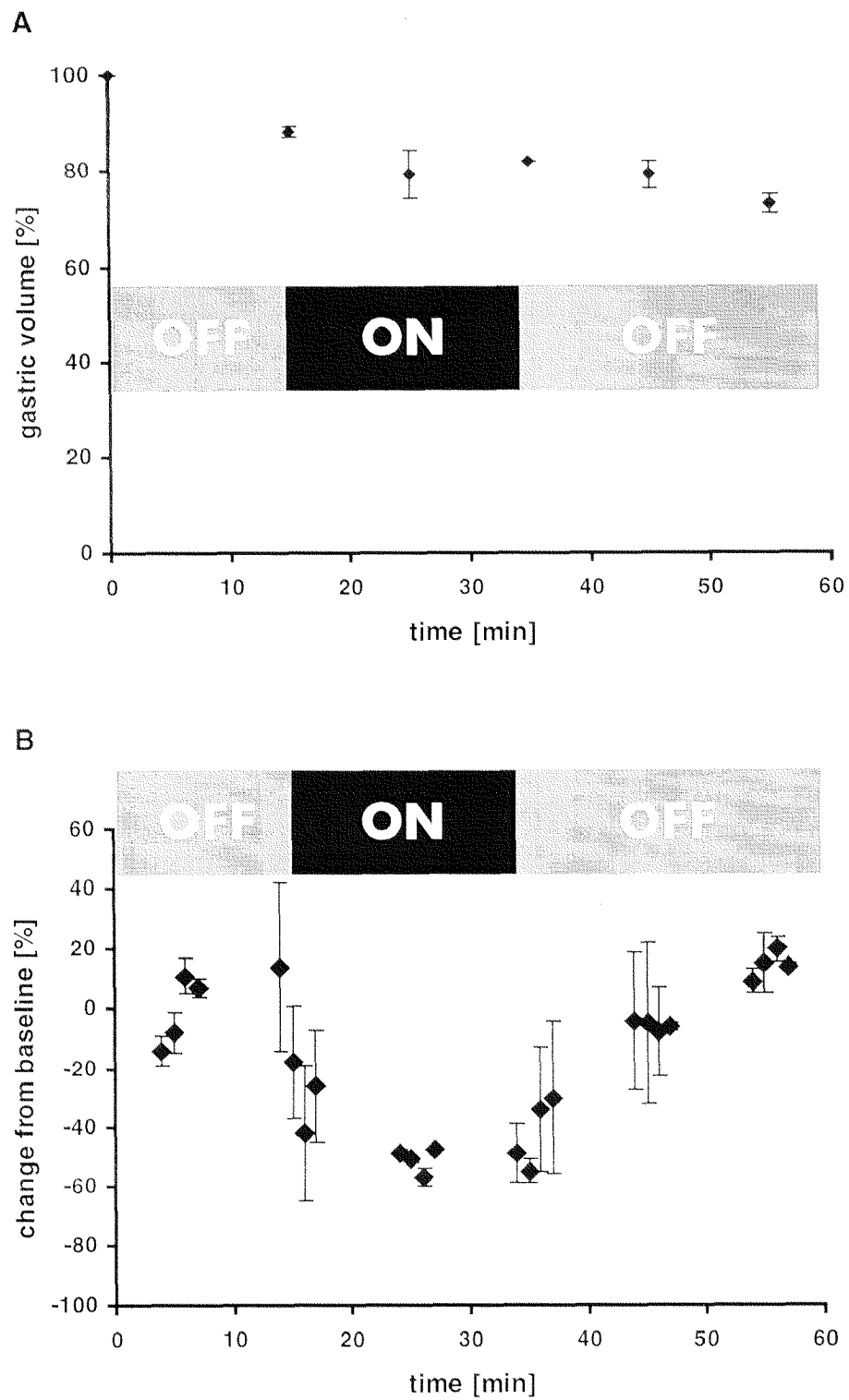
Figure 5: (A)Time course of gastric volume retained in the stomach. (B) Course of the change in contractile strength relative to baseline during the rest – vection – rest paradigm. Antral contractile activity was reduced under vection and returned to baseline following discontinuation of the vection stimulus.

Part 2: paradigm rest – vection – rest

Gastric emptying

Gastric emptying was slowed by the vection stimulus (Figure 5a) and the inhibition persisted after withdrawal of the stimulus.

Contractile strength

The time course of the contractile strength is shown in Figure 5b. After onset of the stimulus, a rapid decrease in antral contractile strength was observed, reaching a change from baseline of -57 ± 3 % at t = 26 min. Recovery of contractile strength started only after a delay. After withdrawal of the stimulus at 35 min, antral contractile strength remained below -10 % change from baseline until t = 42 ± 5 min, and then slowly returned to baseline level.

Discussion

We demonstrated in this study that antral contractile activity was inhibited by optokinetic stimulation. Thereby, antral smooth muscle followed a distinctive time course with respect to the stimulus, characterized by a rapid decrease of contractile strength with the onset and a lag phase after withdrawal of the stimulus, before return to baseline. The intensity of motion sickness symptoms could not be related to the change in gastric emptying or the change in gastric contractile activity.

In order to come to a comprehensive characterisation of the effect of vection on the periphery, it is crucial to identify quantitatively measurable physiological parameters corresponding to changes in physiology in response to the provocative stimulus. Quantification of gastric peristaltic contractions has a number of advantages over previously suggested methods, such as assessment of gastric emptying. The response is immediately apparent, in contrast to the assessment of changes in gastric emptying, which take considerable time to develop as also shown in this study. The ability to quantify an immediate response is especially important for the correlation of the timing

of centrally perceived symptoms with peripheral effects. Since the development of motion sickness is a continuous, dynamic process, it is important to describe the time course of accompanying physiological changes. In order to find possible correlates, symptoms of motion sickness have been assessed in the present study in regular intervals based on subjective reports of the subjects in our study.

What causes the physiological effects and symptoms associated with illusory self-motion and motion sickness is still unclear. Our own findings support the hypothesis that the symptoms of motion sickness and the changes in gastric function are occuring simultaneously, but independent of each other. Previous studies using EGG recordings led to the conclusion that afferent information from the gastrointestinal tract causes the centrally generated symptom of motion sickness [7]. This view was challenged by another group's findings [8], who failed to show a correlation between gastric emptying and motion sickness and could not fully reproduce the EGG findings. This observation complies with our own data and suggests that symptoms of motion sickness and nausea are probably not of a peripheral origin.

The question remains, whether there is a common, central mechanism leading to the great variety of effects observed under vection. The only report on central processing of a vection stimulus showed that vection not only activates bilaterally a parieto-occipital visual area but also deactivates the parieto-insular vestibular cortex [13]. The authors found a positive correlation between the perceived intensity of circular vection and the relative changes in cerebral blood flow in parietal and occipital areas. They concluded that reciprocal visual-vestibular interaction acts as a multisensory mechanism for self-motion perception, shifting the dominant sensorial weight from one sensory modality to the other. It is not clear, however, what changes occur, when this information does not comply with previous sensory experience, provoking Reason's sensory mismatch. According to this model [14], a conflict signal triggers the different mechanisms mediating the symptoms and physiological correlates of motion sickness. It remains to be further investigated, what the central response to vection are and how the theories outlined above can be unified to identify, if possible, a central mechanism underlying the physiological changes observed under vection.

In summary, we have demonstrated the antral motor response to circular vection. This represents an objective physiological parameter, which can be used to investigate the development of the autonomic response during visual – vestibular conflict. However, it appears that antral contractile activity does not represent a suitable predictor for an individual's susceptibility to symptoms of motion sickness.

References

1. Pavlov I. The work of digestive glands. London: Griffin, 1910.

2. Cannon WB. The influence of emotional states on the functions of the alimentary canal. Am J Med Sci 1909;137:480-487.

3. Fone DR, Horowitz M, Maddox A, Akkermans LM, Read NW, Dent J. Gastroduodenal motility during the delayed gastric emptying induced by cold stress. Gastroenterology 1990;98:1155-61.

4. McDonough MC, Schneider M. The effect of motion on the roentgenographic appearance of the stomach and small bowel. Gastroenterology 1944;2:32-45.

5. Wood MJ, Wood CD, Manno JE, Manno BR, Redetzki HM. Nuclear medicine evaluation of motion sickness and medications on gastric emptying time. J Clin Invest 1987;22:877-882.

6. Stern RM, Koch KL, Leibowitz HW, Lindblad IM, Shupert CL, Stewart WR. Tachygastria and motion sickness. Aviat Space Environ Med 1985;56(11):1074-7.

7. Koch KL, Stern RM, Vasey MW, Seaton JF, Demers LM, Harrison TS. Neuroendocrine and gastric myoelectrical responses to illusory self-motion in humans. Am J Physiol 1990;258:E304-10.

8. Reid K, Grundy D, Khan MI, Read NW. Gastric emptying and the symptoms of vection-induced nausea. Eur J Gastroenterol Hepatol 1995;7:103-8.

9. Hu S, Stern RM, Vasey MW, Koch KL. Motion sickness and gastric myoelectric activity as a function of speed of rotation of a circular vection drum. Aviat Space Environ Med 1989;60:411-4.

10. Schwizer W, Maecke H, Fried M. Measurement of gastric emptying by magnetic resonance imaging in humans. Gastroenterology 1992;103(2):369-76.

11. Kunz P, Crelier GR, Schwizer W, Borovicka J, Kreiss C, Fried M, Boesiger P. Gastric emptying and motility: assessment with MR imaging-preliminary observations. Radiology 1998;207:33-40.

12. Muth ER, Stern RM, Thayer JF, Koch KL. Assessment of of the multiple dimensions of nausea: The nausea profile. J Psychosomatic Res 1996;40:511-520.

13. Brandt T, Bartenstein P, Janek A, Dieterich M. Reciprocal inhibitory visual-vestibular interaction. Visual motion stimulation deactivates the parieto-insular vestibular cortex. Brain 1998;121:1749-58.

14. Reason JT. Motion sickness adaptation: a neural mismatch model. J Royal Soc Med 1974;71: 819-829.

Chapter 5

Intragastric distribution of a colloidal drug model in humans – an MRI study

H. Faas[1], T. Rades[2], C. Feinle[3], H. Lengsfeld[2], C. de Smidt[2], P. Boesiger[1], M. Fried[3], W. Schwizer[3]

[1] Biophysics Division, Institute of Biomedical Engineering and Medical Informatics, University and ETH Zurich, [2] F. Hoffmann-LaRoche, PRNF, Basel, [3] Department of Gastroenterology, University Hospital Zurich, Switzerland

Abstract

There is an increasing need to control release of a drug from a specific galenic preparation in the human gastrointestinal tract. The aim of the present study was to investigate the intragastric distribution of a colloidal drug model (liposomes containing the contrast agent Gd-DOTA) by magnetic resonance imaging (MRI). Following ingestion of a liquid or a solid meal, the gastric distribution of liposomes released from a capsule and the fat component of the solid meal were tracked in 7 healthy subjects for 90 min. Liposomes were identified in gastric content by the increased signal intensity provided by the encapsulated Gd-DOTA. With the liquid meal, liposomes initially formed a layer on the surface before distributing in 86 ± 2 % of gastric content (maximum distribution volume) within 42 ± 6 min. With the solid meal, maximum distribution (7 ± 1 %, reached within 24 ± 6 min) was confined to a small volume in the fundus without forming a layer, suggesting that distribution was related to the accessible liquid compartment. Fat distribution was inhomogeneous and concentrated in the fundus. The intragastric distribution of a colloidal drug carrier model, such as Gd-DOTA-filled liposomes, varies between meals of different composition. These differences can be monitored in three dimensions in humans by MRI.

Introduction

There is an increasing need to control release of a drug from a specific galenic preparation in the human gastrointestinal tract. This is particularly important for drugs that act locally in the gastrointestinal tract[1], if site specific absorption is desired[2], in case of drug-food interactions[3] or in conditions in which release of the drug close to the site of macronutrient digestion is required, as is the case in pancreatic insufficiency and cystic fibrosis[4]. Furthermore, *in vivo* monitoring of dosage forms would allow to establish optimal drug delivery based on data on local release in the GI tract. This information may also be required by regulatory authorities[5].

In humans, gamma scintigraphy has been used successfully to investigate the *in vivo* fate of pharmaceutical dosage forms[5-7]. However, due to the radiation burden involved, this technique cannot be used for extensive studies on healthy subjects. Moreover, no information on the 3D distribution in relation to the anatomy can be obtained. More recently, magnetic resonance imaging (MRI) has been proposed as an alternative or additional tool to gamma scintigraphy to study drug distribution in the gastrointestinal tract[8]. MRI has become an established research tool for the assessment of gastric emptying of liquid and solid meals and gastric motor function[9-14]. So far, only two studies have used MRI to monitor the behavior of a drug model in the gastrointestinal tract. One study in humans investigated disintegration of oil-filled soft gelatin capsules in a water-filled stomach[15]. In another study, the behavior of a tablet given orally was studied in the gastrointestinal tract of a rat using a combination of ^{1}H- and ^{19}F-MRI[16]. However, no investigation has examined the fate of more realistic drug models after release from the dosage form.

The aim of the present study was to investigate the intragastric distribution of a colloidal drug carrier model (Gd-DOTA-labeled liposomes) released from hard gelatin capsules after ingestion of either a liquid or a mixed solid-liquid meal.

Methods

Subjects

Eight healthy subjects (7 male, 1 female) between 21 and 27 years participated in the study. The subjects were not taking any medication prior to or during the study and had no history of gastrointestinal disease. Written informed consent was obtained, and the protocol was approved by the ethics committee of the University Hospital Zurich.

Study protocol

The study consisted of two parts: In part 1, the intragastric distribution of a *colloidal system* (liposomal Gd-DOTA) was examined, in part 2, an aqueous *solution* (Gd-DOTA) was studied for comparison.

Part 1: Eight subjects were allowed a light breakfast before 8.00 am, but no food or drinks except water thereafter and arrived at the unit in the early afternoon. Each subject was studied on two occasions. After ingestion of either a liquid or a solid meal, subjects were positioned in the MR imager in a supine, 30° right angulated position, and a reference scan was performed to map the signal intensity of gastric content. Then, a hard gelatin capsule filled with an aqueous dispersion of liposomally encapsulated Gd-DOTA (Dotarem®, Laboratoire Guerbet, Aulnay-sous Bois, France) as MR contrast agent[17] was ingested. Opening of the capsule and the dynamic distribution of the liposomes was followed over 90 min. MRI scans were performed continuously until release of the colloidal dispersion from the capsule was first observed (t = 0 min), thereafter every 2 min until t = 20 min, then every 5 min until t = 50 min and finally every 10 min until t = 90 min. To trace the distribution of the fat phase of the solid meal, an image of the fat signal was obtained prior to capsule administration, at t = 20 min and thereafter every 15 min until the end of the study. In one subject, opening of the capsule occurred prior to the first scan. The data from this subject were therefore excluded from the analysis.

Part 2: After ingestion of the liquid meal, five subjects ingested a hard gelatin capsule containing Gd-DOTA solution (in contrast to liposomally encapsulated Gd-DOTA in part 1). The distribution of the contrast agent was traced over 60 min.

Liposome preparation

Liposomes are closed vesicles with a bilayer structure enclosing an aqueous compartment, which allows incorporation of hydrophilic MRI contrast agents[18]. Gd-DOTA containing liposomes were prepared as described in detail in appendix 1. In the following, the terms colloidal system, liposomes and drug carrier model are used interchangeably.

Preparation of hard gelatin capsules containing Gd-DOTA-liposomes or Gd-DOTA solution: 670 µl of either the liposomal dispersion (part 1) or the Gd-DOTA solution (part 2) were filled into transparent, closed, sealed hard gelatin capsules (size 0,

nominal volume: 680 µl). After sealing of the injection hole, the capsule was then immediately given to the subjects positioned in the MR imager.

Test meals

500 ml 20 % glucose solution (400 kcal) served as liquid meal. The solid meal (645 g) consisted of a fat-free component (270 g spaghetti, 200 g fat-free tomato sauce) and a fat component (40 g mayonnaise on 35 g toast) and was served together with 100 ml water. The fat component was ingested after the first half of the fat-free meal component. The energy content of the meal was 795 kcal with 53 energy% from carbohydrates, 10 energy% from protein and 37 energy% from fat. The liquid content of the meal was 30 %.

MR Imaging

Examinations were performed with a 1.5 Tesla whole body imager (Gyroscan ACS-NT, Philips Medical Systems, Best, NL). The gastric lumen was imaged by 20 transverse slices covering the region of interest. Acquisition time was 20 s using a multislice spin echo sequence (Turbo Spin Echo; TE/TR = 30/698 ms; flip angle: 90°; 256 * 256 pixels; field of view 440 mm, in-plane resolution: 1.7 * 1.7 mm; slice thickness: 8 mm). The lipid signal (i.e. from body fat or ingested fat) was suppressed prior to imaging by a frequency-selective pre-pulse and subsequent gradient dephasing. For intensity standardisation, all images were referenced to the signal intensity of the liver and an external reference as control. In a different scan, the ingested fat component was selectively imaged ('fat scan') by suppression of the water signal (selective excitation and gradient dephasing of the water signal).

Data analysis

Gastric content was outlined in each image in all 20 slices to obtain the gastric volume at each time point. Gastric emptying was expressed as the percentage of gastric content remaining after 90 min[11].

Histogram analysis: In order to describe the intragastric distribution of the contrast medium (liposomal Gd-DOTA or Gd-DOTA solution), the intensity distributions of

gastric content in the scans were determined in each subject. For statistical analysis, the most frequent signal intensity (i.e. the maximum in the histogram) was chosen and averaged over subjects at each time point.

Maximum intensity projection and homogeneity of distribution: The 3D intensity distribution was visualized in two standard orientations (coronal, transversal) as a maximum intensity projection (MIP). The MIP represents a summary image in which individual pixel signal intensity corresponds to the highest signal intensity encountered along a projection line drawn through all 20 images of a scan perpendicular to the image plane. In this way, the homogeneity, in particular 'hot spots' with high concentrations of the contrast agent or fat, could be visualized.

Distribution kinetics: Intensity histograms allowed discrimination between meal and different intragastric concentrations of the contrast agent using an intensity threshold based on the highest intensity of the reference scan prior to capsule intake. By setting the threshold to the highest intensity of the meal before capsule intake (low threshold), volume elements (voxels) in which Gd-DOTA was present could be identified. In order to determine the distribution of high concentrations of the contrast agent, a second threshold (high threshold) 25 % above the detection threshold was chosen.

Gastric regions: All calculations were done for the whole stomach and for antrum and fundus, which were identified from three-dimensional reconstructions of the stomach and divided at the angula.

Statistical analysis: Data are expressed as means ± SEM. A paired, two tailed t-test was used to test for statistical significance. $P < 0.05$ was regarded as statistically significant.

Results

Liquid meal

Distribution of the liposomes could be followed in all subjects and all time periods. Capsule opening occurred in the fundus on the surface of the liquid meal. Upon release from the capsule in the fundus (2.5 ± 0.6 min after ingestion), its liposomal content rapidly formed a layer on the liquid surface (Figures 1, 2b).
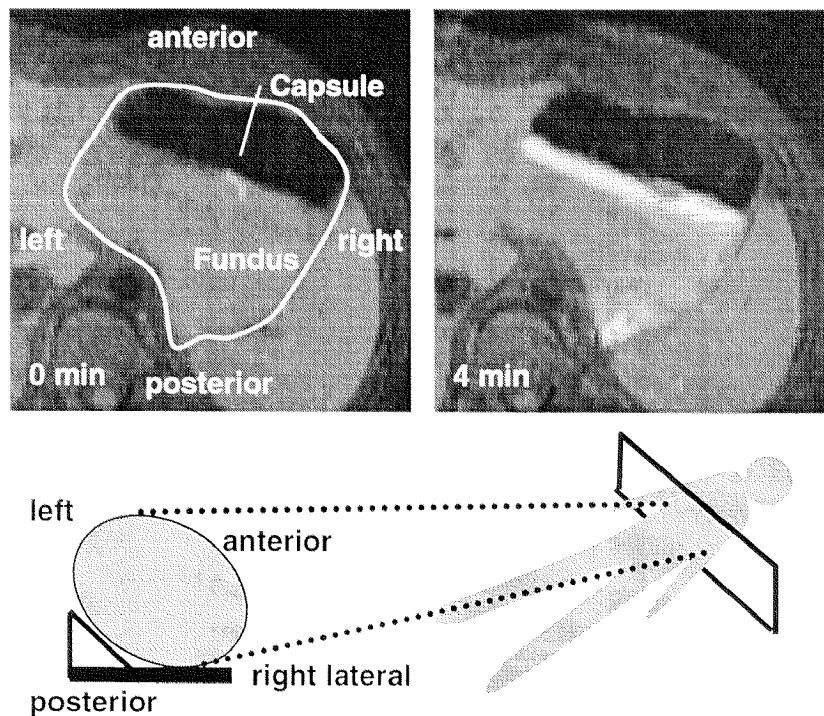

Figure 1: MR images at two time points showing distribution of the liposomes in the fundus after ingestion of a liquid meal. Subjects were in a supine 30° right angulated position. Following release from the capsule, Gd-DOTA filled liposomes provided a high signal intensity in the images.

Figure 2 shows the characteristics of the liposomal distribution in a maximum intensity projection and in the intensity histograms. Immediately after capsule opening, the layer of Gd-DOTA liposomes (Figure 2b) occupied only a small fraction of total meal volume (11 ± 4 % at 2 min after capsule opening), while the single peak in the histogram (Figure 2a) represented the background intensity of the part of the meal that

had not mixed with the liposomes. After this initial period, liposomes covered a larger proportion of the total liquid volume, resulting in a second peak in the histogram at higher intensities (Figure 2a).

At 80 min, the difference between background intensity and liposomes in the histogram had disappeared as shown in the maximum intensity projection (Figure 2 b), indicating a homogenous distribution of liposomes in the liquid meal. After 90 min, 38 ± 11 % of the initial volume was still present in the stomach. Distribution of the liposomes in the entire meal volume reached a maximum (86 ± 2 % of total volume, corrected for gastric emptying) at 42 ± 6 min (Figure 3a).
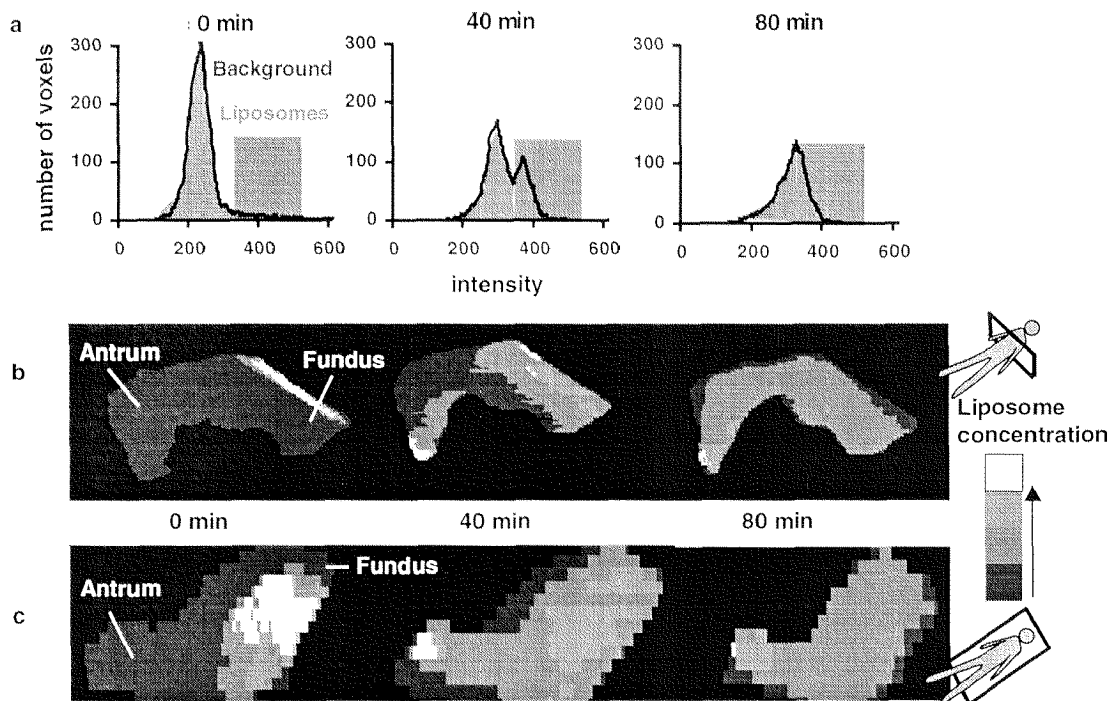

Figure 2: (a) The intensity histograms show the distribution of the liposomes (pink) and the background meal intensity (blue). At intermediate time intervals (40 min), two close but distinct peaks appeared, which eventually merged and resulted in a single peak (80 min) indicating homogeneous distribution. (b) Maximum intensity projection of the liposome distribution in transverse and (c) coronal views: at t = 0 min, opening of the capsule floating on the surface of the liquid and initial rapid layering of the liposomes on the surface was observed, followed by distribution first in the fundus and finally, a near-homogeneous distribution.

Subsequently, the distribution volume decreased again to 55 ± 10 %. To assess the inhomogeneity of the liposomal distribution, a second – high – threshold (25 % above the lower) was chosen, to identify voxels with a higher concentration of liposomes.
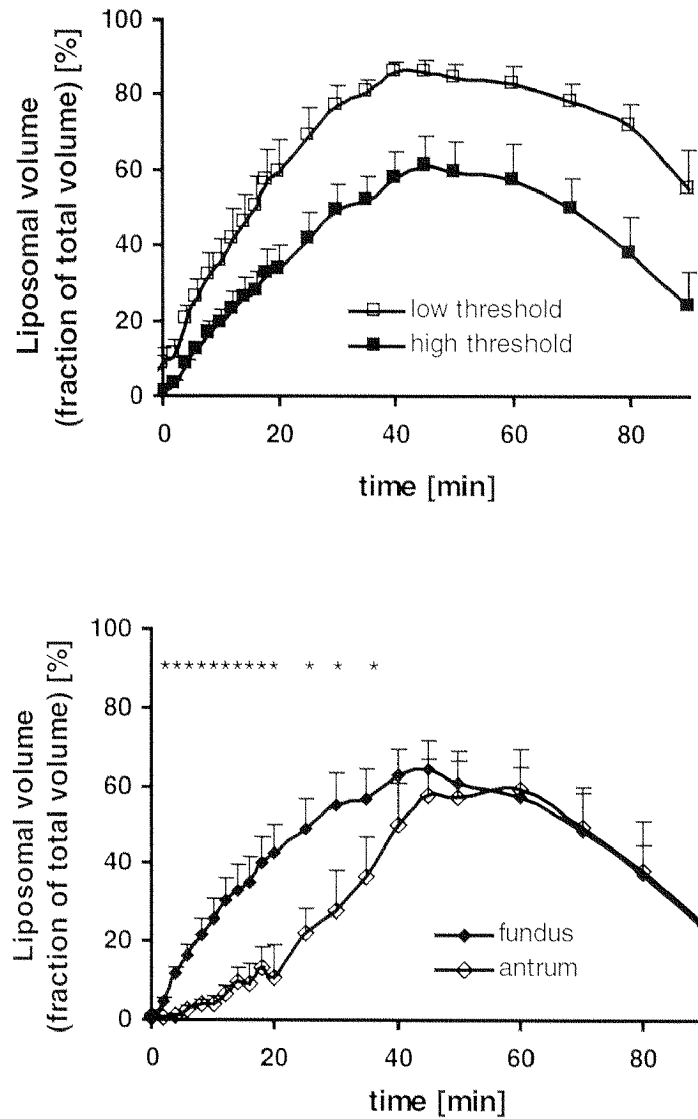

Figure 3: (a) Kinetics of distribution of the colloidal system in the liquid meal at two detection thresholds (high and low). (b) Distribution of higher liposome concentrations (high detection threshold) occurred faster in the fundus than in the antrum until 40 min. Thereafter, no difference was found between the two gastric regions. Asterisks indicate significant difference between distributions at each time point.

This high threshold revealed that distribution of higher concentrated liposomes occurred faster in the fundus than in the antrum until 40 min ($p < 0.05$, Figure 3b),

resulting in an early distribution of liposomes in the fundus. Liposome distribution into the antrum was slow until 20 min after capsule opening (antral distribution volume increasing by 6 ± 3 % per 10 min). After that time, distribution into the antrum was faster (antral distribution volume increasing by 31 ± 10 % per 10 min, $p < 0.05$) until maximum distribution was reached. Thereafter, no difference was found between the two gastric regions.

Solid meal

The liposomal preparation and the fat component could be visualized in the solid meal in all subjects (Figure 4). Figure 5 shows a maximum intensity projection of the liposomal distribution in the solid meal. Capsule opening (3.0 ± 0.7 min after capsule intake) occurred in the fundus, where a high liposome concentration was observed in all subjects around the gastro-esophageal junction. The site, where liposomes were concentrated, remained stationary throughout the study period (Figure 5b). In contrast to the liquid meal, no layering was observed. Distribution of the liposomes was confined to a small volume, which is shown by the fact that no prominent 'liposomal' peak was found in the histograms (Figure 5a) and that the intensity of the meal (the maximum of the main peak in the histogram in Figure 5a) was not shifted towards higher intensities. After 90 min, 67 ± 5 % of the initial volume was still present in the stomach.
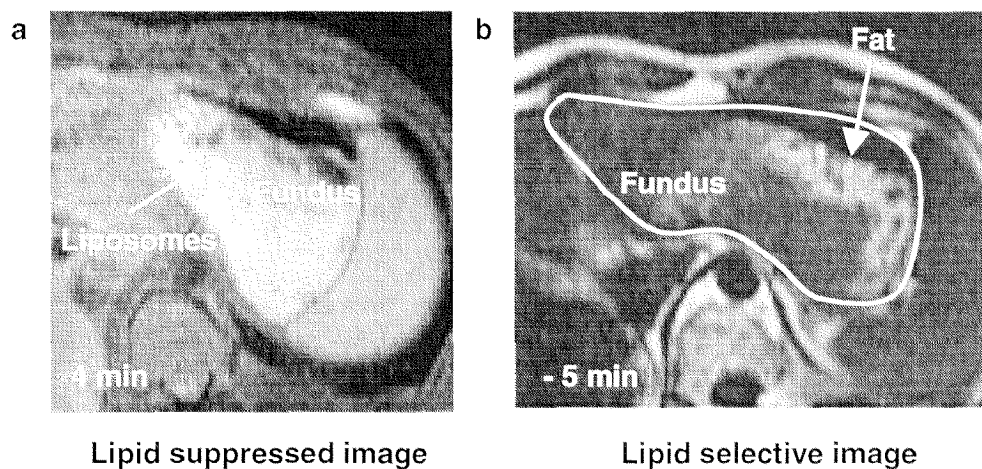

| Lipid suppressed image | Lipid selective image |

Figure 4: MR image showing the distribution of the colloidal drug model (a) and dietary fat (b, before capsule intake) in the fundus after ingestion of the solid meal.

Maximum distribution of the liposomes in the entire meal volume was reached after 24 ± 6 min, faster than the liquid meal (p < 0.05) The liposome distribution reached a plateau of constant distribution volume within 12 ± 2 min and 33 ± 8 min of 1 % of the maximum value. Maximum distribution volume (obtained with the low threshold) was much lower (7 ± 1 %) compared with the liquid meal (p < 0.05; Figure 6).
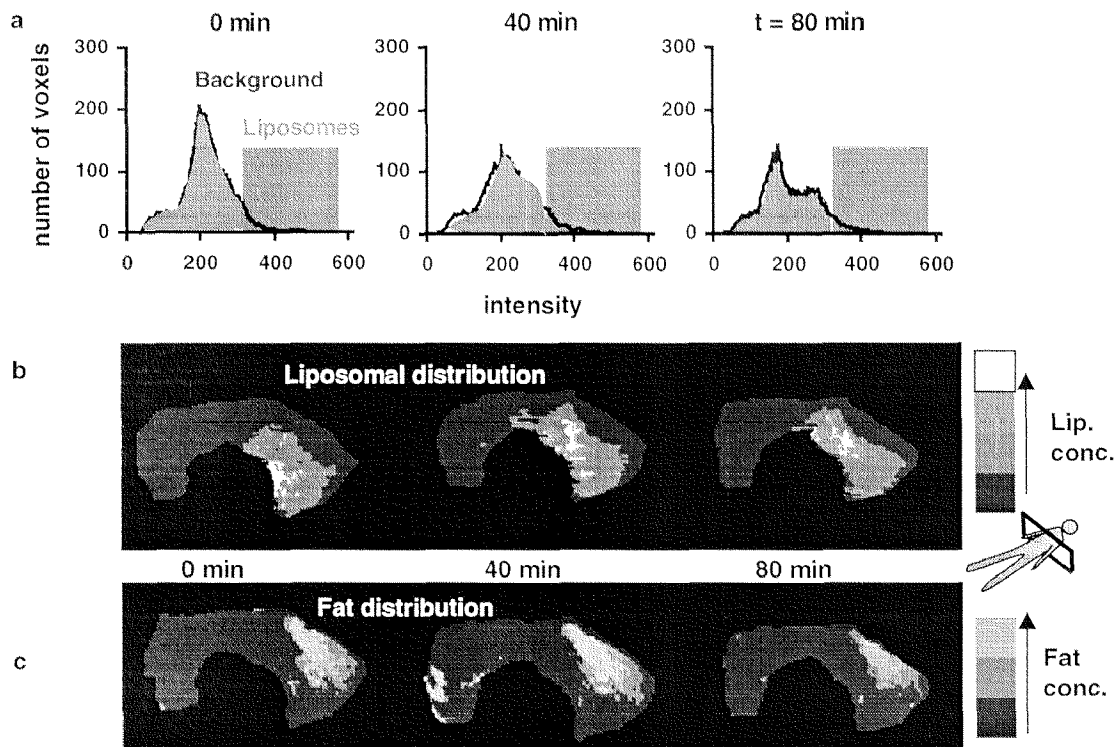

Figure 5: Intragastric distribution of liposomes containing Gd-DOTA after ingestion of the solid meal. (a) The histograms show no distinct signal peak attributable to the colloidal system indicating confinement to a small volume. (b) Maximum intensity projection of the liposome distribution in transverse view. A 'hot spot' with a high concentration of liposomes in the fundus remained stationary over the study period. (c) Maximum intensity projection of the fat distribution. The largest part of the fat was located at a site different from the liposomal 'hot spot'.
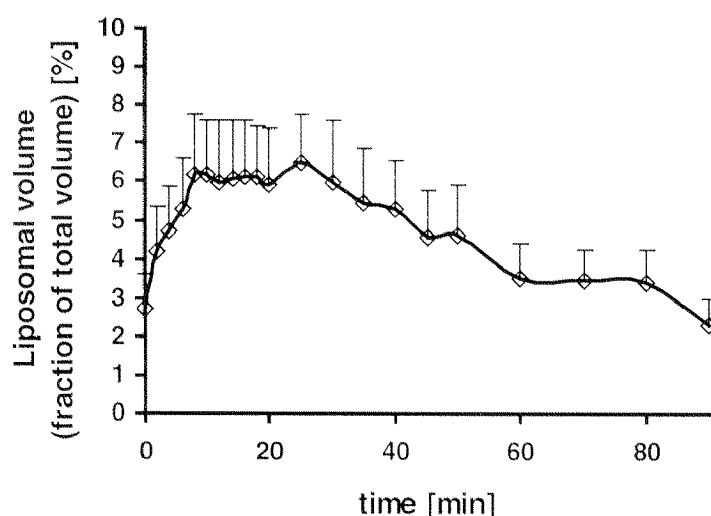
Figure 6: Kinetics of the liposomal distribution in the solid meal. Distribution of the liposomes was confined to a small volume.

Fat distribution: In all subjects, the distribution of the dietary fat could be clearly identified. Fat distribution was highly inhomogeneous, as shown in the maximum intensity projection plots (Figure 5c). The largest part of the fat was located close to the surface forming a layer at a site different from that of the liposomes over the entire 90 min.

Gd-DOTA solution: To compare the maximum distribution volume of liposomes with the distribution volume of an aqueous solution, the liposomal content of the ingested capsule was replaced by a Gd-DOTA solution in a separate experiment. The maximum distribution volume of the Gd-DOTA *solution* in the solid meal was found to be 29 ± 2 %, compared with only 7 ± 1 % for the *liposomal* preparation.

Discussion

The distribution of a drug in the GI tract strongly affects both its systemic bioavailability as well as local availability. In this study, we examined by MR imaging the intragastric release and distribution of Gd-DOTA-filled liposomes, representing a colloidal drug carrier model, in relation to different meal phases.

Our study has shown that the intragastric distribution of the colloidal drug model depends substantially on the physicochemical characteristics of meals. Ingestion of a capsule containing liposomally encapsulated Gd-DOTA after the liquid meal resulted in an almost complete distribution of the drug model into gastric content within about 40 min. Layering of the liposomes, the main process in the first minutes after capsule opening, may be explained by the density difference between the liquid meal and the colloidal dispersion (see Appendix 1). However, once the colloidal system had begun to mix with part of the gastric content, its subsequent homogenous distribution in the total volume could not be attributed to density differences or a passive diffusion process (Appendix 2). Hence, an active distribution process, convection, was most likely responsible for the distribution of the colloidal system in the liquid meal. The predominant movement was directed towards the antrum, presumably following the flow of gastric content caused by gastric emptying. Mechanical factors such as gastric contractile activity, breathing or cardiac motion are likely to be important for the mixing process in the stomach[19]. Antral peristaltic activity could explain the fact that distribution in the antrum was initially slow, then rapidly increased until maximum distribution was reached. Once the formulation was within the reach of the antral peristaltic contractions, liposomes would be rapidly distributed the over the antrum. Influx of gastric secretion may also have contributed to the distribution of the drug model, leading to additional convection along the gastric wall. By reducing the signal intensity, dilution of the liposomal Gd-DOTA concentration by gastric secretion is likely to be responsible for the decrease in distribution volume after the maximum had been reached.

Distribution of the drug model after ingestion of a solid meal was confined to a small volume, indicating that substantial parts of gastric content were not accessible to the colloidal system. Comparison of the distributions between the two meals showed that the liposomes occupied almost the entire gastric volume in case of the liquid meal, but only a fraction in case of the heterogeneous solid meal. To investigate whether distribution may be restricted to the liquid compartment of the meal, we followed the release of a Gd-DOTA *solution*, which was expected to readily distribute into the accessible liquid volume. In fact, its distribution corresponded to the estimated volume of aqueous compartment of the solid meal. In contrast, the *colloidal system* was found

to cover only a quarter of the volume compared with the solution. A reason for this discrepancy may be that liposomes interact differently with meal components inhibiting access to the entire aqueous compartment. In spite of this difference, the large difference in distribution volumes between liquid and solid meals suggests that the colloidal drug model distributed into the accessible aqueous compartment of gastric content.

We also assessed the intragastric distribution of the fat component of the solid meal and of the liposomal distribution in relation to dietary fat. The fat contained in the meal used in our study did not distribute homogeneously within the solid phase, but remained largely stationary throughout the study period. Earlier studies have shown that the intragastric distribution of a liquid fat is primarily controlled by gravity[20]. The distribution of a drug carrier especially in relation to the fat components of a meal may have substantial consequences for the bioavailability of drugs[3]. For example, enzymes acting intraluminally, e.g. affecting fat digestion in chronic pancreatic insufficiency or cystic fibrosis, rely on the simultaneous arrival of enzyme and fat in the small intestine[21]. We observed a spatial separation between the sites of the fat and the drug model, which persisted over the course of the study period, demonstrating that drugs in the stomach are not necessarily well mixed with dietary fat. These results emphasize the need to investigate the intragastric distribution process of colloidal drug carriers with a wide range of 'physiological' meals.

Our method as any other imaging technique faces two technical challenges: the selectivity for the drug model against background 'noise' (e.g. the meal and surrounding viscera) and the sensitivity of the method to low concentrations of the MR marker. One approach to address the issue of selectivity is the use of double contrast techniques as shown in animal studies[15, 22], in which the fluorine content of an intact capsule was visualized by imaging ^{19}F in addition to the standard water (^{1}H) MR image. Despite the higher selectivity of the double contrast technique, this method has not yet been employed in humans, due to its insufficient sensitivity. In contrast, our technique takes advantage of the enhanced signal intensity of the water protons in the vicinity of Gd-DOTA molecules. The contrast enhancement of the colloidal system (liposomal Gd-DOTA) was lower than that of Gd-DOTA alone, due to the shielding

effect of the lipid bilayer. With regards to sensitivity, the reduced contrast effect of liposomal Gd-DOTA compared with Gd-DOTA solution may lead to underestimation of the total volume occupied, but nevertheless allows to study the relevant distribution characteristics. An advantage of this technique is that it can readily be transferred to standard clinical MR scanners. Thus, MRI studies to investigate interactions of different dosage forms with various meals become feasible. The method is not restricted by radiation burden, has a high resolution and provides 3D information. In addition, it is possible to directly assess the relationship between drug distribution, gastric emptying and motility.

In summary, we have demonstrated that MRI allows investigation of the intragastric distribution of a colloidal drug model in humans after ingestion of different meals. Our data indicate that in a liquid gastric content, an active redistribution process is the main mechanism underlying distribution of a colloid. In a solid meal, colloids only enter a fraction of total meal volume, suggesting that distribution occurs mainly in the accessible aqueous compartment. To improve the efficacy of orally administered drugs, detailed knowledge of the behavior of complex pharmaceutical delivery systems in the gastrointestinal tract is mandatory. MR techniques, such as the method described in this study, may help to achieve this goal.

Appendix 1

Preparation of meglumin gadoterate (Gd-DOTA) liposomes

An ethanolic solution of 4.5 g soya phosphatidylcholine was placed into a round bottom flask. The solvent was removed by rotary evaporation under reduced pressure at 40 °C. The lipid film obtained was hydrated for 60 min in 30 ml of a Gd-DOTA solution to which 270 mg sodium chloride had been added and vortexed until the entire lipid film was removed. The resulting multilamellar vesicle dispersion (soya phosphatidylcholine concentration: 150 mg/ml) was transferred into a pressure filter device (Sartorius Membranfilter, Göttingen, Germany) and extruded under nitrogen pressure through 47 mm polycarbonate filters of defined pore size (Nuclepore, Pleasanton, CA., USA). Extrusion was performed twice through filters with 400 nm

pore size (pressure: 3.5 bar), twice through 200 nm (5 bar), and twice through 100 nm (8.5 bar). Hydrodynamic radii and polydispersity index (PI, ranging from 0 = homogenous to 9 = heterogeneous) of the liposomal dispersion were measured by quasi elastic light scattering (Nano-Sizer PSM 78, Coulter Electronics, Krefeld, Germany). Hydrodynamic radii were found to be 153 ± 5 nm (n = 6), and PI was determined to be 3. The Gd concentration was determined by energy dispersive x-ray fluorescence (EDXRF, Spectro X-Lab, Spectro GmbH, Cleve, Germany) and was found to be 7.3 %. To separate free from liposomally entrapped Gd-DOTA, 1 ml aliquots of the liposomal dispersion were dialysed against 1 litre 0.9 % sodium chloride solution using a Lipoprep-GD-1 instrument (Diachema AG, Rüschlikon, Switzerland). After 1 hour, the dialysate was replaced by 1 litre of fresh 0.9 % sodium chloride solution. Samples were removed from the dialysis cell after a total dialysis time of 2 hours. Hydrodynamic radii and polydispersity index of the liposomal dispersion after dialysis were 158 ± 3 nm (n = 6), and PI = 2-3. The Gd concentration was determined with EDXRF and was found to be 0.42 % (entrapment efficiency: 5.8 %). To increase the Gd-DOTA concentration in the liposomal dispersion, the pooled dispersions after dialysis were filled in 1 ml tubes and centrifuged in a Beckman TL-100 ultracentrifuge (Beckman Instruments International, Basel, Switzerland), rotor: TLA-45, speed: 40.000 r.p.m. (100.000 g), time: 30 min, temperature: 15 °C, deceleration from 5.000 to 0 r.p.m. in 4 min). Approximately 600 µl of the clear supernatant in the tubes were removed, the remaining content was pooled and vortexed. Hydrodynamic radii and polydispersity of the liposomal dispersion after ultracentrifugation were 157 ± 2 nm (n = 6), and PI = 2-3. The Gd concentration was determined with EDXRF and was found to be 0.90 %. The liposomal dispersions were stored at 4 °C for no longer than 2 days before being used in the study. In preliminary experiments using EDXRF, it was found that more than 97 % of the Gd-DOTA remained encapsulated in the liposomes for 2 days of storage at 4 °C. Incubating the lipsomal dispersion for 2 hours in human gastric juice (pH 4), aqueous 20 % glucose solution or a 1:1 (v/v) mixture of human gastric juice and glucose solution at 37 °C did not lead to a change in the average size of the liposomes (determined by elastic light scattering) or measurable leakage of Gd-DOTA from the liposomes (determined by EDXRF after ultracentrifugation of the dispersion). The density at 37 °C of the liposomal dispersion (not of the liposomes) was determined to be 1.02, the density of the 20 % glucose solution 1.07.

Appendix 2

Influence of gravity and diffusion on distribution of colloids

Due to their colloidal particle size (diameter 150 – 170 nm), liposomes do not sediment as a result of gravity, since Brownian motion (i.e. diffusion) would override sedimentation. The role of diffusion in the distribution process can be estimated by calculating the diffusion pathway ($x = (6 \, D \, \Delta t)^{-1}$) for three dimensional diffusion. With a diffusion coefficient D of approx. $2.5 \ 10^{-12} \ m^2 \ s^{-1}$ (calculated from the Stokes-Einstein equation, $D = kT/6\pi\eta r$, with k: Boltzmann constant, T: temperature in Kelvin, η: viscosity of the glucose solution and r: radius of the liposomes), the distance liposomes would have passed solely due to diffusion in 90 min is only 0.3 mm, far less than the distribution observed in our study. Thus, diffusion (based on Brownian motion) can also be ruled out as a major factor underlying the distribution phenomena observed in this study.

References

1. May HA, Wilson CG, Hardy JG. Monitoring radiolabeled antacid preparations in the stomach. Int J Pharm 1984;19:169-176.

2. Rouge N, Buri P, Doelker E. Drug absorption sites in the gastrointestinal tract and dosage forms for site-specific delivery. Int J Pharm 1996;136:117-139.

3. Charman WN, Porter CJH, Mithani S, Dressman JB. Physicochemical and physiological mechanisms for the effects of food on drug absorption: The role of lipids and pH. Int J Pharm Sci 1997;86:269-282.

4. Bruno MJ, Haverkort EB, Tytgat GNJ, Van Leeuwen DJ. Maldigestion associated with exocrine pancreatic insuffiency: Implications of gastrointestinal physiology and properties of enzyme preparations for a cause-related and patient-tailored treatment. Am J Gastroenterol 1995;90(9):1383-93.

5. Davies SS, Hardy JG, Newmann SP, Wilding IR. Gamma scintigraphy in the evaluation of pharmaceutical dosage forms. Eur J Nucl Med 1992;19:97-986.

6. Wilson CG, Washington N. Assessment of disintegration and dissolution of dosage forms in vivo using gamma scintigraphy. Drug Dev Ind Pharm 1988;14:211-281.

7. Wilding IR, Coupe AJ, Davies SS. The role of gamma scintigraphy in oral drug delivery. Adv Drug Deliver Rev 1991;7:87-117.

8. Wilson CG, McJuryM, O'Mahony B, Frier M, Perkins AC. Imaging oily formulations in the gastrointestinal tract. Adv Drug Deliver Rev 1997;25:91-101.

9. Schwizer W, Fried M, Maecke H. Measurement of gastric emptying in humans by magnetic resonance imaging. Gastroenterology 1992;103:369-376.

10. Feinle C, Kunz P, Boesiger P, Fried M, Schwizer W. Scintigraphic validation of a magnetic resonance imaging to study gastric emptying in humans. Gut 1999;44:106-111.

11. Kunz P, Crelier GR, Schwizer W, Borovicka J, Kreiss C, Fried M, Boesiger P. Gastric emptying and Motility: Assessment with MR Imaging – Preliminary observations. Radiology 1998;207:33-40.

12. Schwizer W, Fraser R, Borovicka J, Asal K, Crelier G, Kunz P, Boesiger P, Fried M. Measurement of proximal and distal gastric motility with magnetic resonance imaging. Am J Physiol 1996;271:G217-22.

13. Boulby P, Gowland P, Adams V, Spiller RC. Use of echo planar imaging to demonstrate the effect of posture on the intragastric distribution and emptying of an oil/water meal. Neurogastroenterol Motil. 1997; 9(1):41-7.

14. Boulby P, Moore R, Gowland P, Spiller RC. Fat delays emptying but increases forward and backward antral flow as assessed by flow-sensitive magnetic resonance imaging. Neurogastroenterol Motil. 1999;11(1):27-36.

15. O'Mahony B, McJury M, Wilson CG. Use of MRI to study the behaviour of soft gelatin capsules in the upper gastrointestinal tract. Proc Soc Magn Reson 1995;3:1475 (abstract).

16. Christmann V, Rosenberg J, Seega J, Lehr CM. Simultaneous in vivo visualisation and localisation of solid oral dosage forms in the rat gastrointestinal tract by magnetic resonance imaging (MRI). Pharm Res 1998;14:1066-1072.

17. Schwizer W, Fraser R, Maecke H, Siebold K, Funck R, Fried M. Gd-DOTA as a gastrointestinal contrast agent for gastric emptying measurements with MRI. Magn Reson Med 1994;31(4):388-93.

18. Tilcock C, Unger E, Cullis P, MacDougall P. Liposomal Gd-DTPA: Preparation and characterisation of relaxivity. Radiology 1989;171:77-80.

19. Hausken T, Odegaard S, Gilja OH, Berstad A. Mixing of gastric contents is evoked by heart contractions and respiration. Neurogastroenterol Mot 1998;10(5):453 (abstract).

20. Edelbroek M, Horowitz M, Maddox A, Bellen J. Gastric emptying and intragastric distribution of oil in the presence of a liquid or a solid meal. J Nucl Med 1992;33(7):1283-90.

21. Fried M. Chronic pancreatitis: treatment of pancreatic insufficiency and pain. In: Acute Pancreatitis: Novel concepts in biology and therapy (Editor: Büchler MW, Uhl W, Friess H, Malfertheiner P). Blackwell Wissenschafts-Verlag GmbH, Berlin 1999: 509 – 512.

Chapter 6

Discussion and outlook

"Life depends on innervation of the viscera, in a way all the rest is biological luxury". While the view of Nauta and Feyrtag [1] seems extreme, it may well have an element of truth. In recent years, research in the field of autonomically regulated processes - cardiac, respiratory or digestive functions - has intensified, with a scope beyond the development of therapeutical strategies, aiming to address more fundamental questions. While research efforts rapidly head towards ever smaller units - individual nerves and molecules - this reductionist approach clearly has its limitations.

The present work adopts an integrative viewpoint when looking at the control mechanisms of gastric motor function. Gastric smooth muscle activity exemplifies the general features of autonomic functions: a number of constantly running, unconscious tasks controlled via feedback mechanisms and modulated by central nervous and humoral mechanisms. Our strategy was therefore to look at gastric smooth muscle activity, as a direct response to the neural and humoral input and then study this system under different stimuli.

MRI offers unique opportunities for investiagting the physiology of the GI tract. With specialized techniques as developed for this work, a high versatility can be achieved, allowing the assessment of a number of parameters such as volume and motility and the possibility to perform interactive real time imaging. Whether MRI can play a role in clinical diagnostics of gastric function will depend on the further extension of the different aspects of the technique, which sets it apart from conventional cheaper methods.

A major regulatory mechanism of gastric motor activity is the duodenal feedback that controls nutrient delivery to the small intestine. Precisely how this information is integrated and on which pathways it is relayed back to control gastric smooth muscle activity is not known. Our approach was to apply a peripheral stimulus (the lipid infusion into the duodenum) and directly measure the activity of the major gastroduodenal motor components that work together to adjust the outcome variable, in our case gastric emptying. Further studies using the combination of manometry and imaging will make use of pharmacological manipulation to focus on the role of the sympathetic nervous system and the relationships and possible compensatory effects between individual motor components. In addition, current efforts aim to create a computer model of the mechanisms responsible for gastric motor function, using as input the biomechanical data from the in vivo studies [2].

Communication between the brain and the gut connects the most distant parts of the regulatory system controlling gastric motor function. In our study of illusory self-motion, the peripheral response to an external stimulus was assessed, disregarding the – yet obscure – cascade of events in between. It appears that stressful motion stimuli influence the stability of autonomic regulatory mechanisms. A next step could be the combination of fMRI with the presented method to assess central and peripheral effects of illusory self-motion. This would help to clarify why the reciprocal inhibitory interaction between visual and vestibular cortex is not sufficient to avoid the sensory mismatch thought to underlie the development of motion sickness.

While processes in the stomach go for the most part unnoticed, unusual activity such as noxious stimuli may cause conscious involvement. This visceral sensation is of great importance to a wide variety of pathophysiological conditions, but the underlying mechanisms are largely unknown. For example, there is increasing evidence that the condition of functional dyspepsia is the result of an abnormal perception of normal events rather than a normal perception of abnormal events in the gastrointestinal tract. Different studies indicate that physiological stimuli of various mechanical and chemical natures are perceived by the patients at a lower intensity than in healthy subjects [3]. It is, however, still unclear where this amplification of the stimulus intensity occurs, and several possibilities exist. The sensitivity of the receptors located in the gastric or gut

wall may have changed, changes may have taken place on the nervous pathways between the gut and the brain, or even within the brain itself. Figure 1 shows an example from our own preliminary work, in which the cortical response to an intragastric mechanical distension stimulus was assessed by functional magnetic resonance imaging. In response to the peripheral stimulus, there is a clear, bilateral activation of the insular region, an important gateway for visceral sensory information, and activation in the prefrontal cortex.
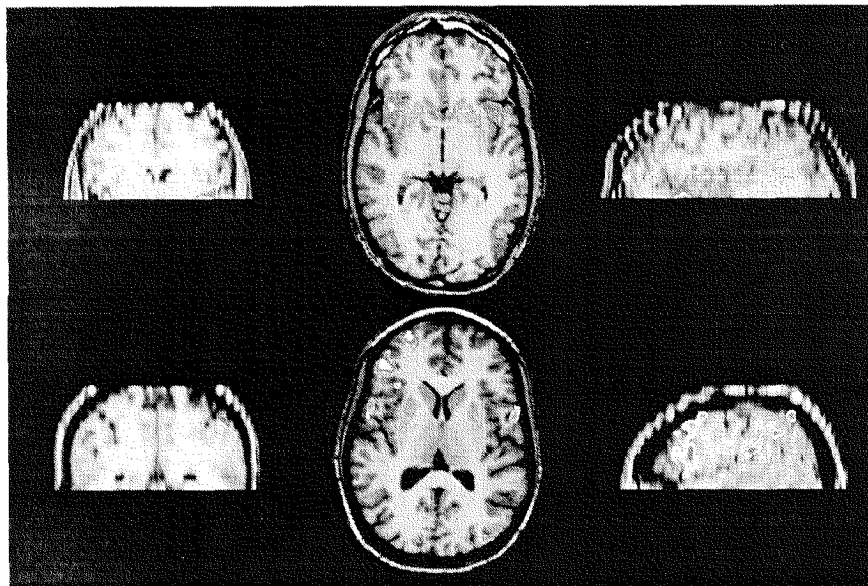

Figure 1: Cortical response to an intragastric distension stimulus.

In conclusion, this work has focused on gastric function as a model autonomic system. Magnetic Resonance Imaging can play a valuable role in improving our understanding in this area. Ultimately, this can be expected to lead to optimized therapeutical strategies and identification of targets for new drugs. Furthermore, monitoring of drug distribution in the gastrointestinal tract gives drug developers a tool to search for optimal galenic forms with improved dose - response relationships.

References

1. Nauta WJH, Feyrtag M. Fundamental neuroanatomy. Freeman, New York, 1986.

2. Indireshkumar K, Pal A, Schwizer W, Hebbard GS, Faas H, Dent J, Chen S, Kunz P, Fried M, Boesiger P, Brasseur JG. Influence of antral contraction waves on intragastric pressure, fluid motions and mixing. Neurogastroenterol Mot 1999;11:267(abstract).

3. Hamdy S, Aziz Q, Rothwell J, Singh K, Barlow J, Hughes D, Tallis R, Thompson D. The cortical topography of human swallowing musculature in health and disease. Nature Medicine 1996;11:1217-1224.

Curriculum vitae

Henryk Michael Faas, born January 25th 1970 in Karlsruhe, Germany

Education

1976 - 1989	Max-Planck Gymnasium, Karlsruhe, Germany
1986 - 1987	Exchange student, Gainesville, Texas, USA
1989	High- School Graduation (University entrance qualification)

Higher Education

1990 - 1993	Undergraduate studies in Physics, University of Karlsruhe, Germany
1993 - 1996	Undergraduate studies in Physics, ETH Zurich, Switzerland
1995	Exchange student, NTH Trondheim, Norway
1995 - 1996	Diploma thesis, Institute of Biomedical Engineering, ETH Zurich
1996	Diploma in Physics, ETH Zurich
1997	Research stay, Pennsylvania State University, USA
1996 - 1999	Doctoral (PhD) thesis, Biophysics Division, Institute of Biomedical Engineering, ETH Zurich, Switzerland